

N O T I C E

THIS DOCUMENT HAS BEEN REPRODUCED FROM
MICROFICHE. ALTHOUGH IT IS RECOGNIZED THAT
CERTAIN PORTIONS ARE ILLEGIBLE, IT IS BEING RELEASED
IN THE INTEREST OF MAKING AVAILABLE AS MUCH
INFORMATION AS POSSIBLE

AS03040R1

January, 1981

(NASA-CR-161846) DESIGN OF A LASER SYSTEM
FOR INSTANTANEOUS LOCATION OF A LONGWALL
SHEARER Final Feasibility Study Report
(Adjunct Systems, Inc.) 99 p HC A05/MF A01

N81-31607

Unclas
35199

CSSL 081 G3/43

DESIGN OF A LASER SYSTEM
FOR INSTANTANEOUS LOCATION
OF A LONGWALL SHEARER

Technical Report
Submitted by

ADJUNCT SYSTEMS
222 Price Alley
P.O.Box 10016
Huntsville, Alabama 35801



The work reported herein was conducted under contract NAS8-34185 with National Aeronautics and Space Administration, Marshall Space Flight Center, Alabama, 35812. The results and opinions do not necessarily represent the official positions of that agency.

AS

TABLE OF CONTENTS

<u>Section</u>	<u>Page</u>
1. INTRODUCTION.....	1
1.1 <u>REVIEW OF CONCEPT</u>	3
1.2 <u>SENSOR SYSTEM CONSIDERATIONS</u>	5
2. LASER BEAMS AS REFERENCES (TASK #1)	10
2.1 <u>TARGETS</u>	10
2.1.1 <u>Laboratory Reflectance Measurements of Coal</u>	11
2.1.2 <u>Published Measurements for Coal Reflectance</u>	13
2.1.3 <u>Calculated Particle Distribution for Coal Dust</u>	18
2.1.3.1 Trajectory Sized Particles	18
2.1.3.2 Suspended Particles of Coal	19
2.1.4 <u>Inferences From Photographs</u>	21
2.1.5 <u>Reflectance From Water</u>	22
2.1.5.1 Radiometric Measurements .	22
2.1.5.2 Photographic Measurements	29
2.2 <u>INTERVENING MEDIUM</u>	32
2.3 <u>ILLUMINATORS</u>	33
2.4 <u>TRADE CALCULATIONS</u>	36
2.4.1 <u>Available Light From Coal Dust</u>	36
2.4.2 <u>Available Light From Water Stream</u> .	37
2.5 <u>IN-MINE EXPERIMENTAL APPARATUS</u>	38
3. SENSOR SYSTEM OPTIONS (TASK #2)	42
3.1 <u>BACKGROUND</u>	42
3.2 <u>INTERVENING MEDIUM</u>	42
3.3 <u>OPTICS</u>	43
3.4 <u>ANALYZERS</u>	45
3.5 <u>TARGET SCAN</u>	45
3.6 <u>BACKGROUND SCAN</u>	46
3.7 <u>DETECTORS</u>	47
3.7.1 <u>Detector Size</u>	48
3.7.2 <u>Irradiance at Detector</u>	49
3.7.3 <u>Detection Signal-To-Noise Ratio</u> ...	50
3.7.3.1 Type I Detector	55

<u>Section</u>	<u>Page</u>
3.7.3.2 Type V Detector	56
3.8 <u>ELECTRONICS</u>	57
3.9 <u>OUTPUT DATA OPTIONS</u>	63
4. SHEARER LOCATION SYSTEM (TASKS #3 and #4)	64
4.1 <u>LIGHT SHAFT TECHNIQUE GEOMETRIES</u>	65
4.1.1 <u>Single Laser Case</u>	66
4.1.2 <u>Two Laser Case</u>	66
4.1.3 <u>Three Laser Case</u>	67
4.1.4 <u>Shafts versus Points</u>	69
4.2 <u>TARGET PLANE TECHNIQUE GEOMETRIES</u>	69
4.2.1 <u>One Point on a Plane</u>	70
4.2.2 <u>Two Points on a Plane</u>	71
4.2.3 <u>Three Points on a Plane</u>	72
4.3 <u>Z-AXIS DETERMINATION</u>	75
4.4 <u>LOCATION BY SCANNED LASER BEAMS</u>	75
5. CONCLUSIONS & RECOMMENDATIONS	32
5.1 <u>CONCEPT COMPARISONS</u>	80
5.1.1 <u>Z-Location Systems</u>	83
5.1.2 <u>XY-Location Systems</u>	83
5.1.3 <u>Attitude Determining Systems</u>	86
5.2 <u>RECOMMENDED SYSTEM</u>	88
5.3 <u>DATA DISPLAY UNIT</u>	95

LIST OF FIGURES

<u>Figure</u>		<u>Page</u>
1.	Illustration of Longwall Shearing Operation	2
2.	Instantaneous Shear Position Locator Concept	4
3.	Illustration of Water Spray Concept	6
4.	Block of Sensor System Consideration for a Laser System for Location of a Longwall Shearer	7
5.	Arrangement for Measurement of Coal Reflectance ..	12
6.	Results of Reflectance Measurements	12a
7.	Plots of Oil versus Air Reflectances for Various n	14
8.	Published Reflectance as a Function of Wavelength	15
9.	Estimated Particle Size Distribution	20
10.	Photograph Showing Low Visibility of Coal Dust Even at the Shearing Drum	23
11.	Photograph Showing the High Visibility of Water Jets Even at Considerable Distance	24
12.	Schematic of Arrangement For Water Stream Measurements.....	25
13.	Results of Water Stream Measurements.....	27
14.	Arrangement for Photographic Tests.....	30
15.	Example Photographic Results	31
16.	Schematic construction of gallium arsenide laser..	35
17.	Schematic construction of helium neon laser.....	35
18.	Light Source Arrangement for Mine Tests.....	39
19.	Camera Arrangement for Mine Tests.....	39
20.	In-mine Photographic Measurement Set-Up.....	41
21.	Spectral Curves for Type I Silicon Detectors.....	52
22.	Typical Quantum Efficiency as a Function of Wave- length for Silicon Avalanche Photodiode at 298 K.	53
23.	Signal Power and Noise Power as Functions of Photocurrent Gain for a Silicon Avalanche Photodiode.....	54
24.	Recommended Circuit for Type I Photodiode.....	58
25.	Typical Curve for Signal and Noise versus Reverse Bias for a Type I Photodiode with Load Resistance of 100 Megohms.....	59
26.	Typical Noise Frequency Spectrum for Type I at Different Reverse Bias; A=1x1mm, and Load Resistance = 1 Megohm.....	60
27.	Capacitance as a Function of Bias for a Typical Type I Photodiode with A=2x2mm.	
28.	Photocurrent Gain as a Function of Reverse Voltage for a Type V Photodiode.....	62
29.	Sketch of the Toroidal-like Ambiguity Surface for Observations of Points A and B.....	68

Figure

Page

30.	System Block Diagram.....	77
31.	Technique for obtaining angular mirror position, providing laser modulation reference and regulating motor speed.....	79
32.	Synchronization Chart for the various optical outputs.....	80
33. a	Sensor Head Portion of the "Quick Response" Concept.....	92
33. b	The Retroreflector Portion of the "Quick Response" Concept.....	93
34.	Trajectories Showing Misalignments of up to 2-Foot and 5-Foot Respectively.....	94
35.	Overlay of New XZ & YZ Trajectories Showing That Considerable Correction Has Been Obtained.....	94

ABSTRACT

Calculations and measurements have been made for the design of a laser system for instantaneous location of a longwall shearer. Designs have been completed based on the calculations and measurements. These designs, with usual engineering refinements, will allow determination of shearer location to approximately one foot. Additionally, the roll, pitch and yaw angles of the shearer track can be determined to approximately two degrees.

The course of analysis lead away from the original concept based on scattering from coal dust particles to two other approaches. The first is a concept using a small scanned stream of the water already pumped to the longwall face for dust suppression. This technique uses a single silicon sensor system and three gallium arsenide laser beams. It is clear that all OSHA and MSHA requirements can be met with the design. Advantages of the water target system rest not only with improved signal levels, but also with more favorable geometries.

The second new technique is based on an arrangement similar to that employed in aircraft omni-directional position finding. The angle between two points is determined by combining information in an omni-directional flash with a scanned, narrow beam beacon. This approach is preferable to the first two because it maximizes signal levels.

1. INTRODUCTION

In longwall coal mining operations a matrix of tunnels is developed in a coal seam as depicted in Figure 1. Two tunnels, running parallel to one another, are separated a substantial distance by the intervening coal seam. Distances of 500 feet are typical. The longwall shearing machine is placed inside a cross tunnel between the two parallel tunnels. The machine rests on tracks which facilitate its traverse along the face of the wall via mechanical engagement to propel the machine. A trough is associated with the tract having a conveying mechanism to transport coal cut from the longwall face out to an end tunnel and to further conveyances leading to the surface of the mine.

Automation of longwall coal mining requires development of a technique by which the shearer can be instantaneously located at all times. This report summarizes studies to establish the feasibility for techniques based on laser and electro-optical technologies. Guidelines assumed for the analysis include use of off-the-shelf components, the unfavorable environment typified by Table 1 and the need to adhere to regulations put forth by the Occupational Safety and Health Administration (OSHA), and the Mine Health and Safety Administration (MSHA), and other applicable regulating agencies.

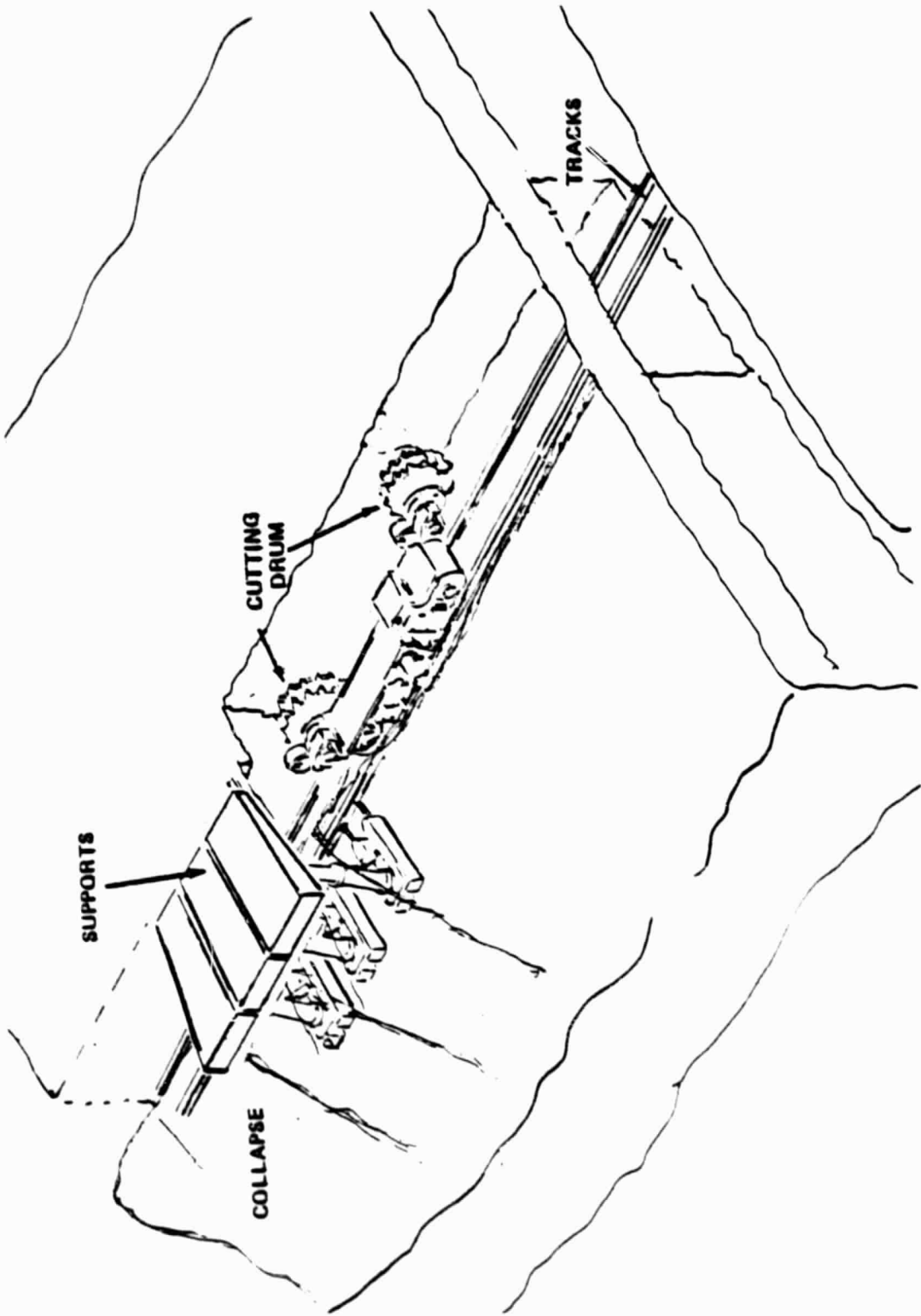


Figure 1 Illustration of Longwall Shearing Operation

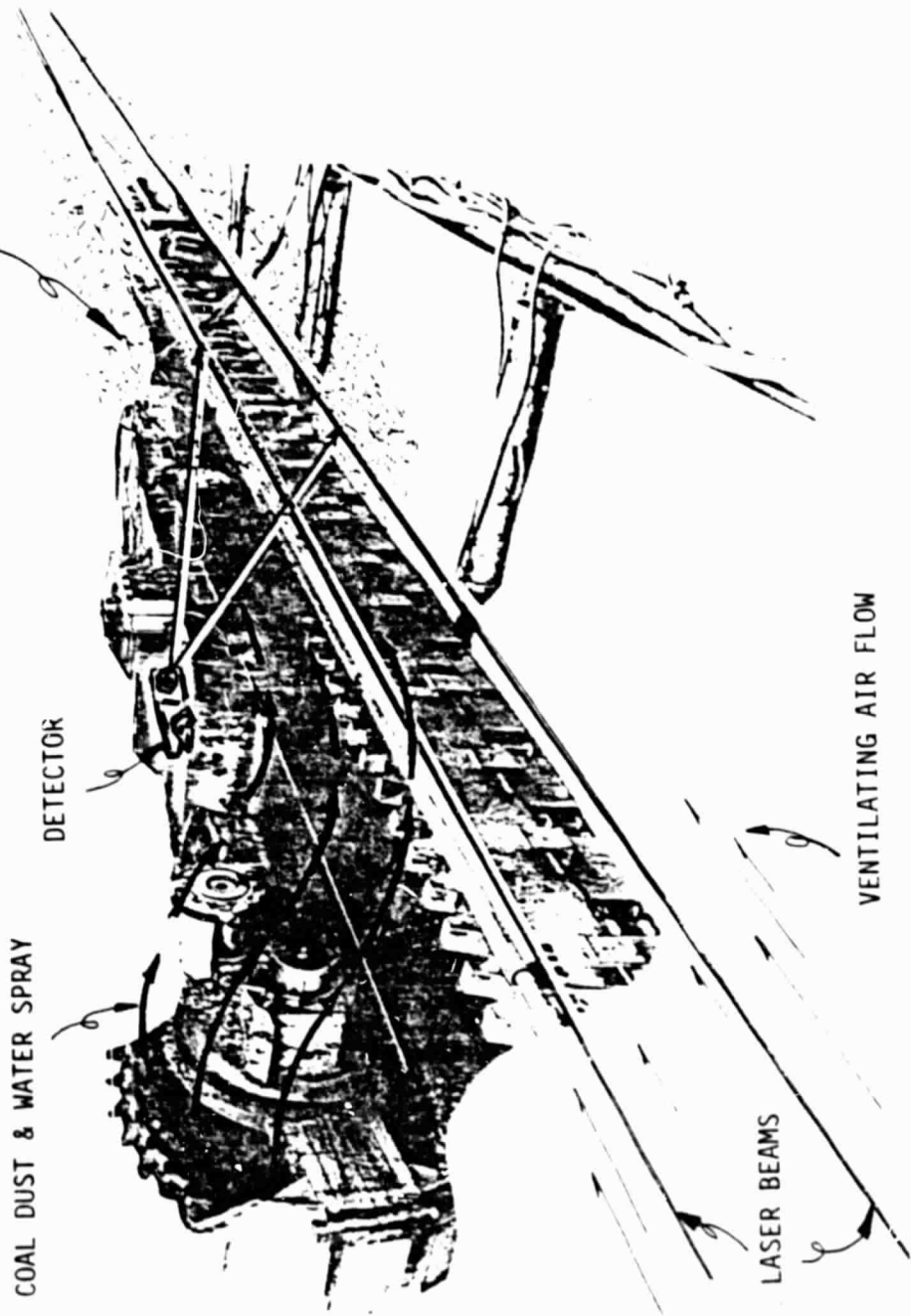
1.1 REVIEW OF CONCEPT

The design concept discussed in this report for instantaneous location of a longwall shearer is based upon the use of laser beams to establish lines of reference. These lines of reference are associated, in their turn, with survey reference at the end of tunnels.

The energy of laser light in a vacuum is propagated in a straight line. Therefore, beams of light directed along the longwall face can be detected only if the observation is made directly on the axis of the beam, or if some imposed material deviates the light's direction. In the case of the coal mine operation, particles of coal dust or water used in dust suppression can serve as potential deviators (scatterers) of the laser light. The scattered light could then be observed from the side by an optical device which would image the illuminated dust onto some form of photo-sensor. This would allow one to see light not originally directed at them. Human experience of the same process is exemplified by dust particles floating through beams of sunlight in an otherwise shaded area.

Figure 2 shows laser beams in the coal dust approach directed alongside the path of the shearing machine. A sensor is mounted on the machine body which monitors the image of coal particles that pass into the beams. The apparent angles between the scattered beams and the machine body provide data from which shearer orienta-

REGION OF HIGH NUMBER DENSITY FOR PARTICULATES



COAL DUST & WATER SPRAY

DETECTOR

LASER BEAMS

VENTILATING AIR FLOW

Figure 2. Instantaneous Shear Position Locator Concept.

AS

tion and position might be determined. The concept is simple, but the realities of implementation can become sophisticated.

Figure 3 shows an arrangement which uses the water spray technique. In this approach the laser beams are not monitored from some perpendicular location. Instead, the beams intersect a plane of water. The intersections appear as bright spots. The sensor is located on the laser side of the water plane, slightly off axis. Actually, as will be explained in later sections, the water plane need not be a continuous sheet. In fact, the preferred design avoids this, using scanned water streams instead. A figure of the scanned laser beam alternative will not be given at this time. It will be introduced more appropriately in Section 4.

1.2 SENSOR SYSTEM CONSIDERATIONS

Figure 4 is a good summary of how sophisticated the design of the longwall sensor system is. This figure portrays, via block diagram, the many interactive elements of the concept analyzed in this design effort. The five general tasks in the design study examine these elements in detail. The results of analysis in each task are presented in each of the main sections that follow this Introduction.

Section 2 presents the results of Task 1 analysis. Activity under Task 1 addresses element blocks #1, #3 and #4 in Figure 4 in order to assess the viability of using a narrow laser beam as a

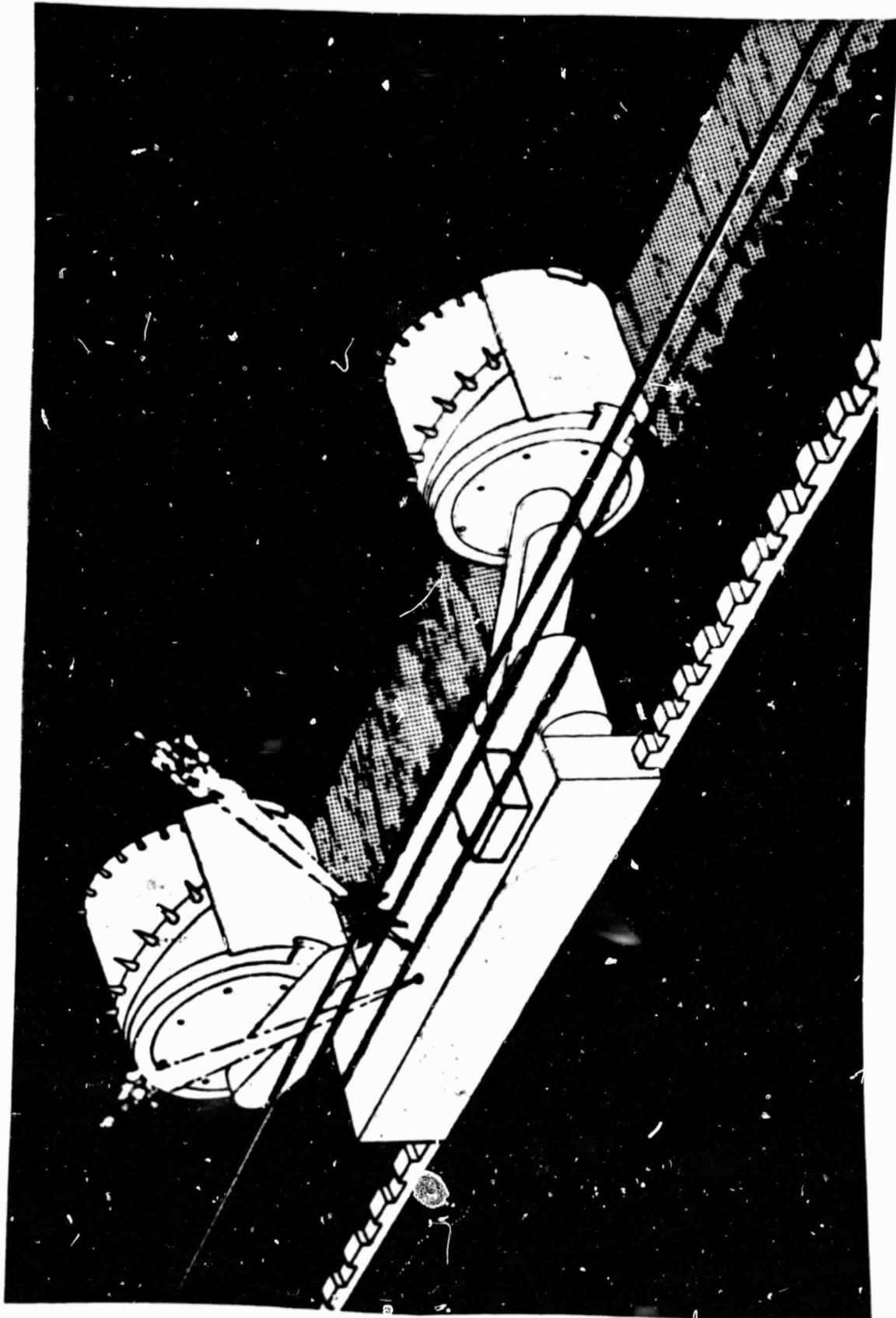


Figure 3. Illustration of Water Spray Concept.

AS

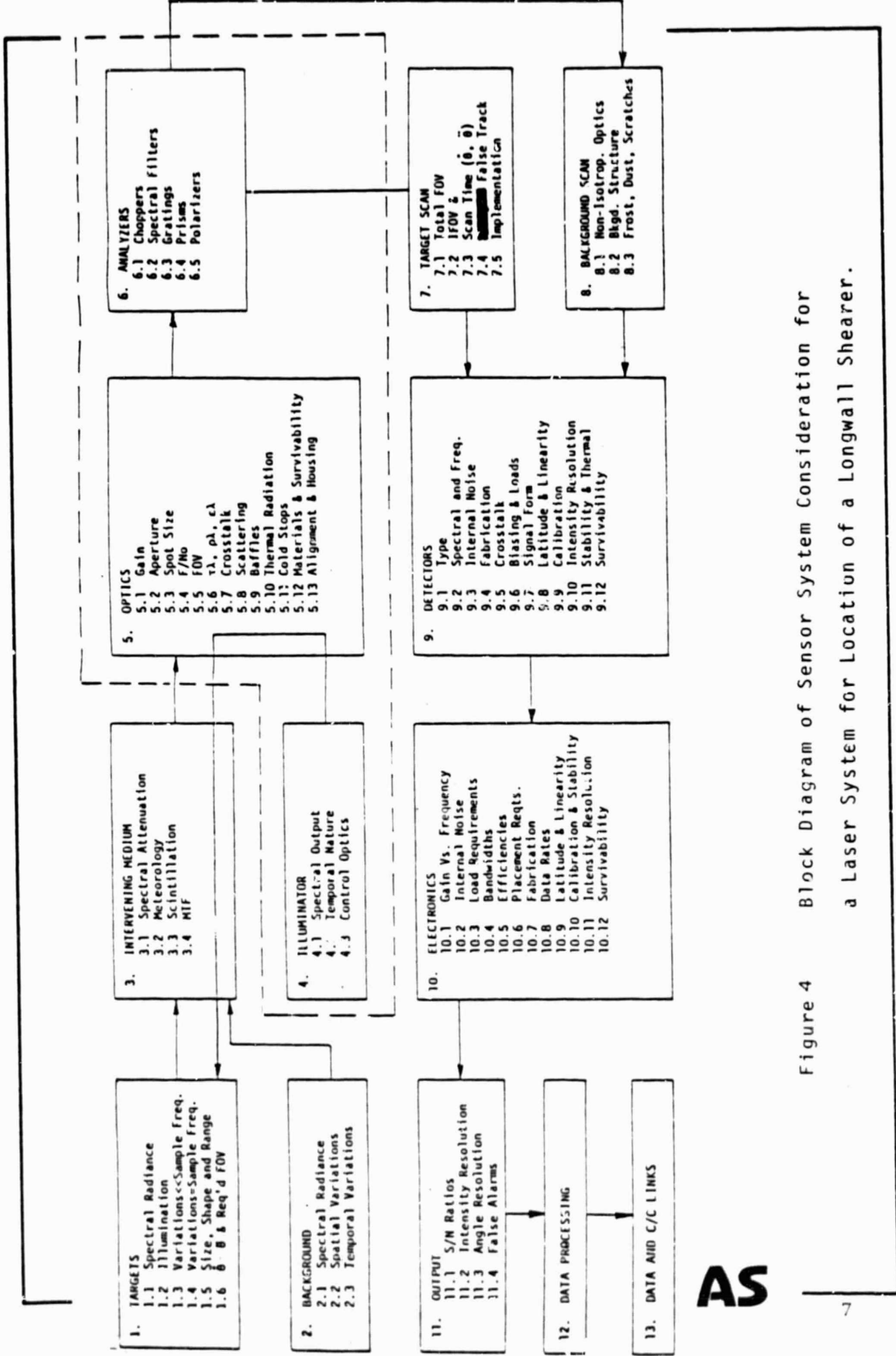


Figure 4 Block Diagram of Sensor System Consideration for a Laser System for Location of a Longwall Shearer.

AS

cross-tunnel reference for determining shearer position.

Task 2, presented in Section 3, uses the results of the first task to determine what sensor system characteristics are needed to observe the laser light scattered by the coal and water particles with a sensitivity and accuracy appropriate to ascertaining shearer location. This task required investigation of elements #2, #3, and #5 through #11.

The results of the first two tasks are incorporated into Task 3, which is presented later as Section 4 of this report. This task addresses the practical realizability of design options when cast into a functioning mine environment. Tasks 4 and 5 extend the design analysis to allow not only location of the shearer, but also determination of roll, pitch and yaw. These tasks are imbedded in the discussions of Section 4.

Section 5 summarizes the findings of the study. The coal particles and water target techniques are compared with each other, and with the scanned laser beam approach. The scanned beam approach is shown to be preferred and an associated first order design is shown.

Shearing Drum Vibration (Supplied by NASA/MSC):

3-10 Hz	0.1 Inch peak to peak
10-30 Hz	0.02 Inch peak to peak
30-300 Hz	1 G Acceleration peak
500-3000 Hz	3 G Acceleration peak

Dust Environment (from Visual Estimates):

Submillimeter particulates propelled by estimated 10 mph air stream along wall at rate providing 100% coverage in estimated 90 minutes at 10m from shearer, 1 minute at 2m from shearer. Potential explosion hazard via electrical spark.

Debris per Square Meter at 2m (from Visual Estimate):

.1 - 1.0 Kg	100 per minute
1 - 5 Kg	20 per minute
7 ⁵ Kg	2 per minute

**Table 1 Environmental Concerns for the
Laser Longwall Shearer Location System**

2. LASER BEAMS AS REFERENCES

(TASK #1)

Effort under Task 1 concentrated on estimation of mine and laser variables to determine if a laser beam can be accurately directed down 600 feet of longwall tunnel, and observed with an arbitrary sensor of ideal performance.

2.1 TARGETS

The targets in this system are coal dust particulates and water droplets. If it were not for these small airborne specks, the presence of a laser beam directed down the tunnel could not be detected from a position perpendicular to the optical axis. It is by virtue of the scattering from the particles that the beam location is possible. In fact, photographs of laser beams used in the laboratory are often made by blowing smoke into the light path.

Several characteristics of these small particles have been examined. Among these are the apparent spectral radiance resulting from laser illumination. This will depend upon several variables, including size, shape and observational fields of view. Additionally, movements of the particles in range and angle over the period of observation are considered with regard to scintillation frequencies. Delineation is made between the absorption and the scattering components of the extinction coefficients, which in turn are related to anticipated particle number densities.

2.1.1 Laboratory Reflectance Measurements of Coal

The arrangement shown in Figure 5 was used by Adjunct Systems to make laboratory measurements of representative coal reflectance. A flat piece of coal had a sheared face set at the center of an indexed rotary table. A gallium arsenide injection diode laser output was collimated with a microscope objective to strike the coal at the center of rotation. The light reflected from the coal face was sampled with a 1-cm² silicon detector placed in the plane that would correspond to specular (mirror-like) reflection. An infrared filter (Wratten 87C) was placed in front of the detector to eliminate the effect of background lights in the visible regions. The detector output was read with an electronic amplifier and meter system calibrated for 0.63um wavelength. The reflectance readings, computed by normalizing to a standard solid angle and to the directly measured output of the laser, is not influenced by the difference in wavelength between the gallium arsenide (0.85um) and 0.65um because both direct and reflected light were measured with the same detector.

The results of the laboratory measurements are shown in Figure 6. The diameter of the light as it struck the face of the coal was approximately 3mm. The coal particles serving as targets in the shearer location concept will be much smaller. Nevertheless, the level of reflectance should be approximately the same in both cases. Only the effective cross sections and directional characteristics are likely to change.

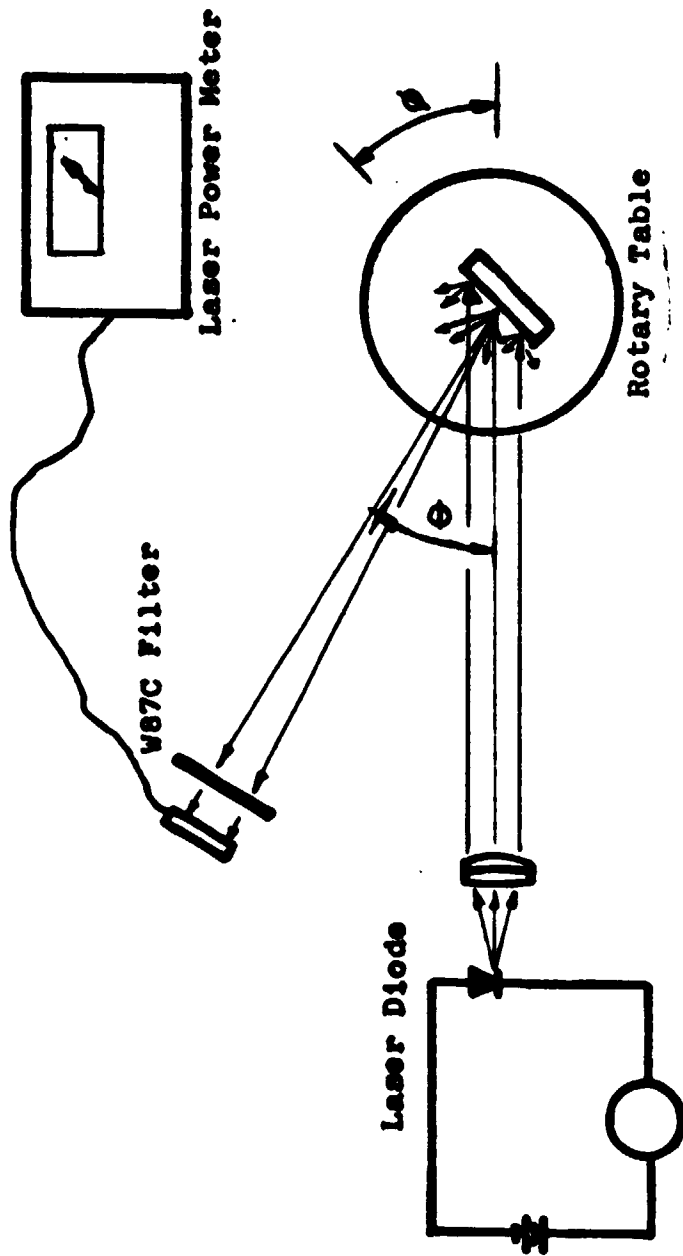


Figure 5. Arrangement for Measurement of Coal Reflectance

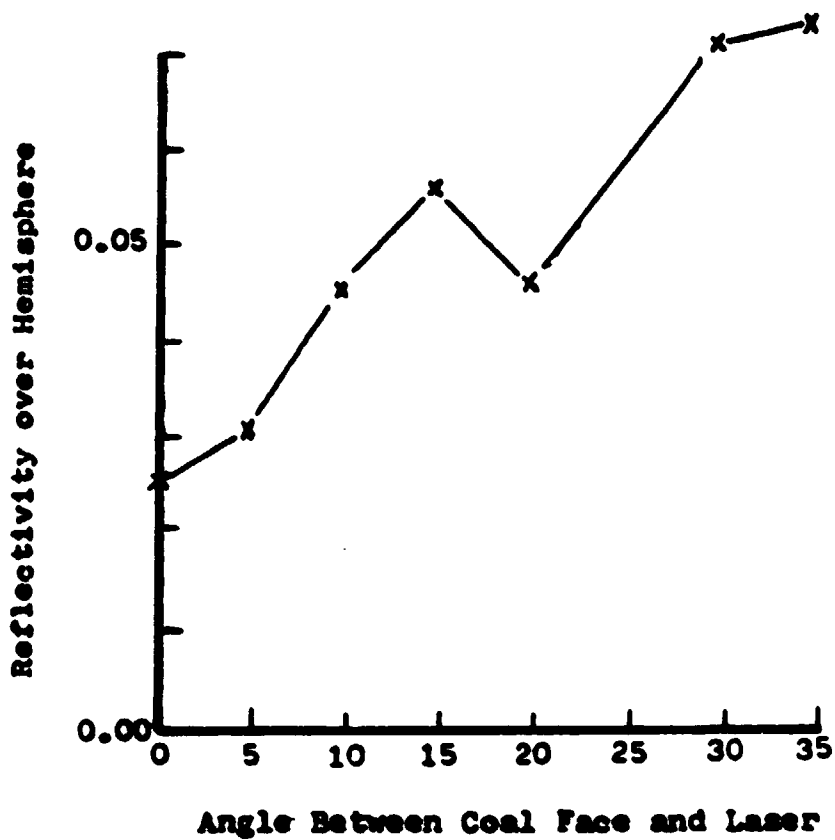


Figure 6. Results of Reflectance Measurements.

2.1.2 Published Measurements for Coal Reflectance

A literature survey was conducted to compare the Adjunct Systems measurements with those of other researchers. It was found that microscopic coal reflectance measurement is an established analytical technique for coal classification. This technique employs oil immersion microscopy of coal polished in a standardized manner. Unlike the Adjunct Systems measurements, which illuminated a sample size of about 3 mm diameter, standard classification techniques observe a spot size of between 5 μ m and 10 μ m. The ASTM standard specifies a 5 μ m diameter. However, measurements at 20 μ m show no loss in accuracy.

Figure 7 shows published measurements of coal reflectance in air and oil as a function of wavelength. It is significant to note that, even though oil and air reflectances are quite different, they vary only slightly with wavelength. Therefore, it is reasonable to expect the reflectance near 0.6 μ m (helium laser) and 0.9 μ m (gallium arsenide laser) will be the same. Comparison of Figure 6 and 7 confirm this to at least a first order.

For a selected wavelength region, the curves of Figure 8 result from data of the Figure 7 type. This is helpful in conversion of the oil immersion reflectance of Table 2 to air reflectances.

The Handbook of Optics provides reflectance data for diffuse hemispherical reflectance of carbon blacks. Table 3 summarizes some of this published data. These are air reflectance values and are in

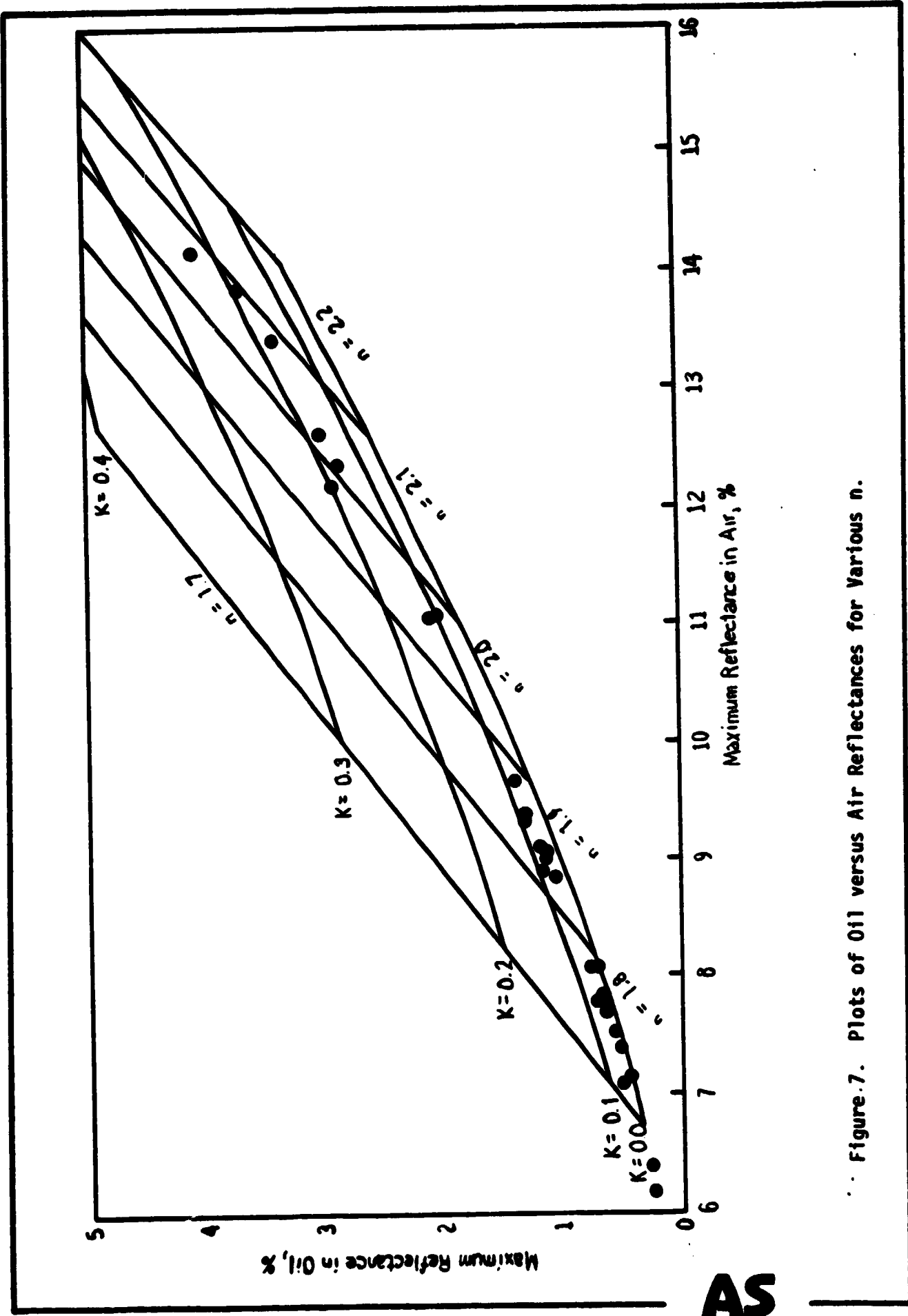


Figure.7. Plots of Oil versus Air Reflectances for Various n .

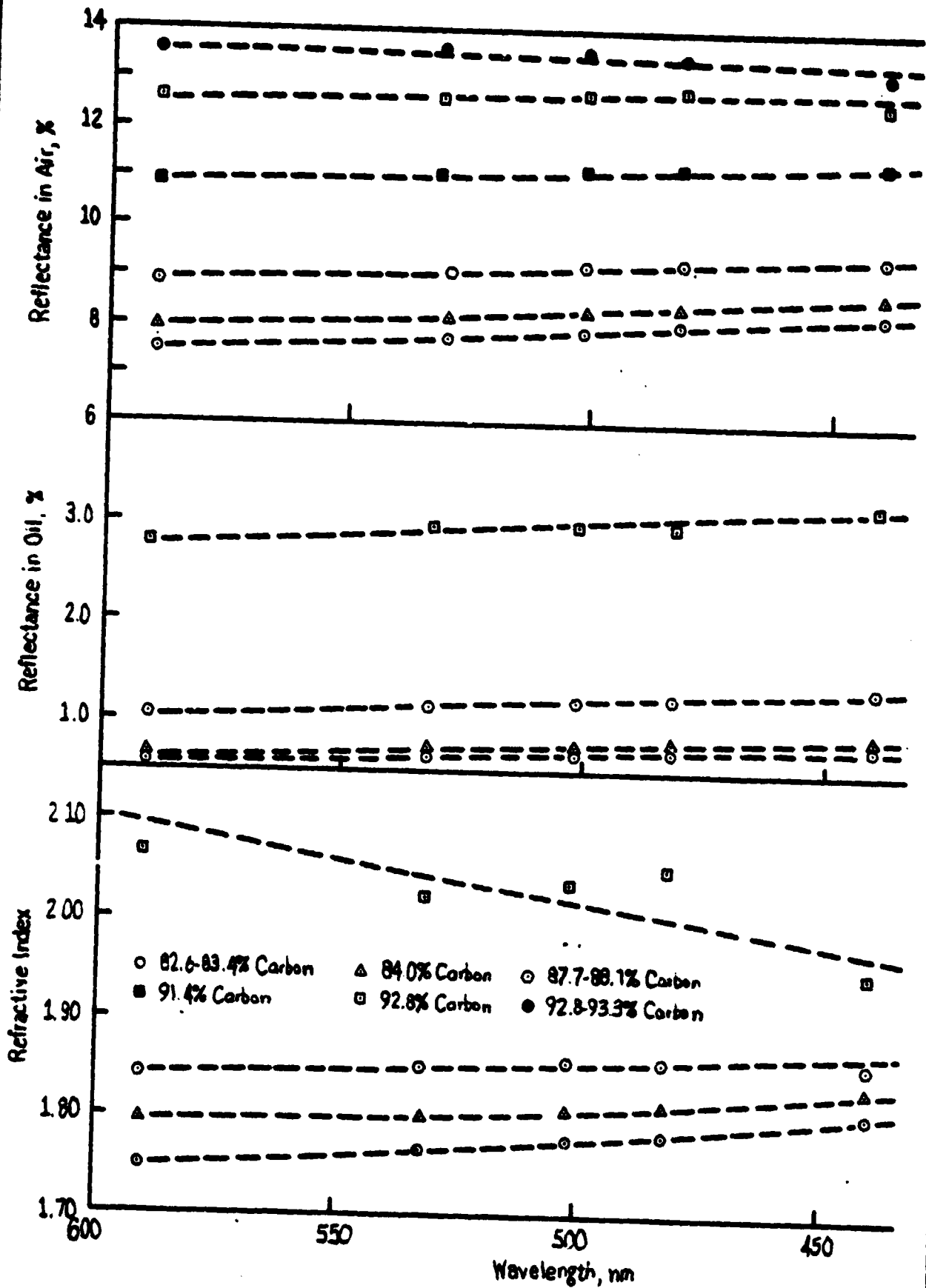


Figure 8. Published Reflectance as a Function of Wavelength.

AS

TABLE 2. PUBLISHED REFLECTANCE DATA

CLASS	RANK	TYPE	MACERAL COMPOSITION (%)			MEAN MAXIMUM REFLECTANCE OF VITRINITE, R_v (%)
			VITRINITE LIPTINITE	FUSINITE SEMIFUSINITE MICRINITE		
ANTHRACITE	META-ANTHRACITE	C	0-50	100-50	>5.0	
		B	50-75	50-25		
		A	75-100	25-0		
	ANTHRACITE	C	0-50	100-50	2.5-5.0	
		B	50-75	50-25		
		A	75-100	25-0		
	SEMANTHRACITE	C	0-50	100-50	2.0-2.5	
		B	50-75	50-25		
		A	75-100	25-0		
BITUMINOUS	HIGH RANK BITUMINOUS	C	0-50	100-50	1.5-2.0	
		B	50-75	50-25		
		A	75-100	25-0		
	MEDIUM RANK BITUMINOUS	C	0-50	100-50	1.0-1.5	
		B	50-75	50-25		
		A	75-100	25-0		
	LOW RANK BITUMINOUS	C	0-50	100-50	0.5-1.0	
		B	50-75	50-25		
		A	75-200	25-0		
	SUBBITUMINOUS	C	0-50	100-50	0.4-0.5	
		B	50-75	50-25		
		A	75-100	25-0		
LIGNITE	LIGNITE	C	0-50	100-50	0.25-0.4	
		B	50-75	50-25		
		A	25-100	25-0		

TABLE 3. DIFFUSE HEMISPHERICAL REFLECTANCE OF CARBON BLACKS

MATERIAL	0.60 μm	0.70 μm	0.95 μm
ACETYLENE BLACK	0.006 & 0.011	0.010	0.004
LAMPBLACK PAINT	0.033	-----	0.047
LAMPBLACK PAINT PLUS SOOT	0.016	0.016	-----
SPERM CANDLE SOOT	-----	-----	0.010

accord with the data mentioned above. The sample areas are large, but the individual particles are small. Based on this, as well as the aforementioned data, it is reasonable to assume that the airborne particles in the longwall tunnel will have reflectances between 3% and 15% over a hemisphere. Furthermore, based on anticipated particle size, scattering of the reflected light should be in all directions.

2.1.3 Calculated Particle Distribution for Coal Dust

The particle size and distribution along the longwall will depend upon several factors. Among these are the proximity to shearers and positions downstream (with respect to ventilation) from the shearing process. The analysis discussed here assumes two conditions prevail. The first condition is dominated by simple equations of motion relating to large object trajectories in a gravitational field. The second condition assumes the prevalence of suspension forces similar in magnitude to those which maintain fog.

2.1.3.1 Trajectory Sized Particles

The assumption is made, for want of other indicators, that the rate of expulsion of sheared particles from the longwall face is constant in mass between the largest and smallest particles. Stated otherwise, if the size of ejecta are multiplied by their number density, the result is a constant with size. Starting with this

assumption, a rough estimate can be made of the particle distribution. Based on review of motion pictures of longwall operations and typical shearer performance data it appears reasonable to estimate that a shearer might produce up to 100 Kg/sec of cut coal. Of this amount, only a few milligrams are likely to be small enough for suspension in air. The rest are trajectory type particles which will quickly fall to the floor. The distribution with distance will depend primarily on the ratio of particle projected area-to-mass ratio. This suggests the carrying power rapidly moving ventilating air will have on it. The suspended particles are also diluted in accordance with the airflow rate. These suspended particles are the principle targets for the laser beams.

2.1.3.2 Suspended Particles of Coal

Optics of the Atmosphere provides a number density curve for various water droplet sizes in atmospheric fog. This general distribution must be modified, however, for the difference between the density of water and the density of coal. The Handbook of Chemistry and Physics gives the density of carbon (graphite) as 2.25g/cm^3 . The cube root of the reciprocal of this value is 0.76, which is the factor adopted in producing the number density plot of Figure 9 from the fog water droplet data.

The area under the curve in Figure 9 was numerically integrated and divided by the total particle number to estimate the diameter of the average particle. This was done to simplify estimates of

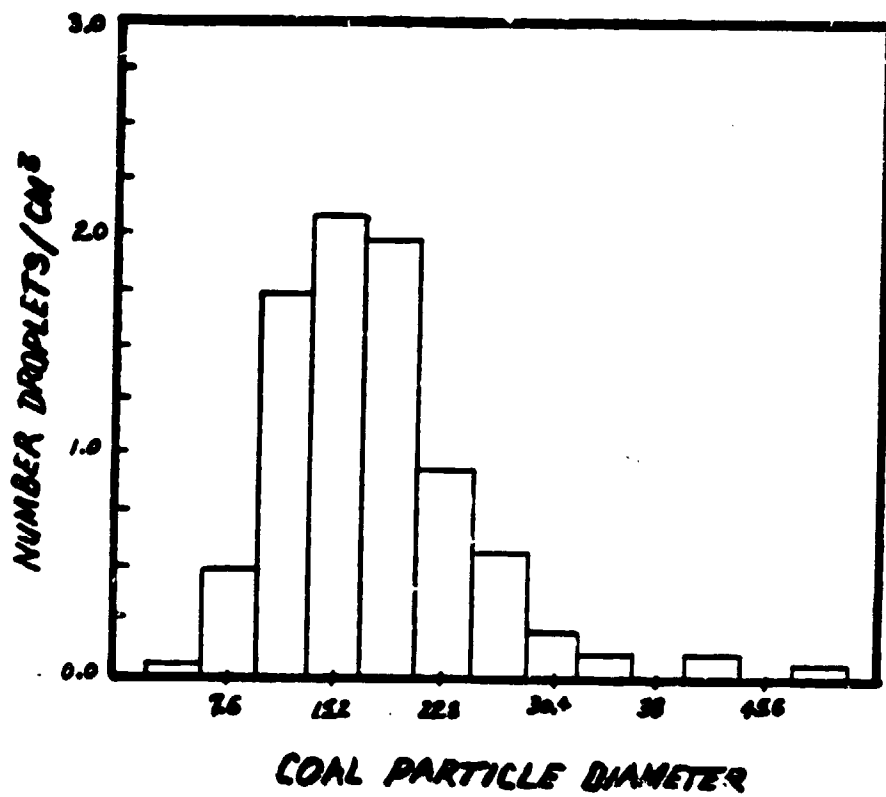


Figure 9. Estimated Particle Size Distribution.

attenuation coefficients. Such estimates should be reasonably accurate as starting values. The average diameter calculated in this manner is 17.6 um. Assuming a spherical particle, the average particle mass is calculated to be 6.4×10^{-9} grams.

The MSHA health standard for respirable particles (maximum) in the coal mine environment is $2\mu\text{g}/\text{m}^3$. Dividing the aforementioned average particle mass into this standard leads to a maximum of approximately 1 particle/ cm^3 . This value is based upon the definition of respirable particle being greater than 10um in diameter. From the distribution of Figure 9, roughly 27% of the suspended particles will be of this category. The number of respirable particles allowable can be calculated from:

$$\# \text{ respirable particles} = \frac{\text{MSHA Standard for particles}/\text{cm}^2}{\text{calculated mass of } 10\mu\text{m particle}}$$

This leads to:

$$0.3/0.27 = 1 \text{ particle}/\text{cm}^3$$

These values will be used later in Section 2.2 to compute the attenuation of a beam of light passing along the longwall suspended particle path, as well as in Section 2.4 where scattered intensity and attenuation per unit pathlength are estimated.

2.1.4 Inferences From Photographs

Motion picture photographs (16mm) were examined using a data analysis projector. Line action showing a longwall shearer in operation were reviewed on a frame by frame basis. Pertinent frames were locked in stop action. The following observations were made.

- (a) Space beyond a few feet of the shearing drum had so few particles as to make their detection improbable without highly sensitive photodetection systems.
- (b) The water streams used for dust suppression are highly visible.

Figure 10 is a photographic print from the cine action film showing the low visibility of coal dust. Figure 11 shows a similar photograph in which water jets are present.

2.1.5 Reflectance From Water

Another target possibility exists along the longwall tunnel. Water sprays are used for suppression of dust let fly by the shearing process. In an effort to examine the potential for water as a target, both radiometric and photographic observations were made. These are related in the following discussion. It is quite significant to note that the use of water as target material affords far greater control, with less health hazard, than coal particles.

2.1.5.1 Radiometric Measurements

Measurements were made of the influence of water streams on a helium laser beam. The arrangement used is shown schematically in Figure 12. The stream was formed by gravity fall from a standard faucet. The laser beam diameter at intersection with the stream was approximately 1.0mm full width, half power. Detection was made

ORIGINAL PAGE IS
OF POOR QUALITY

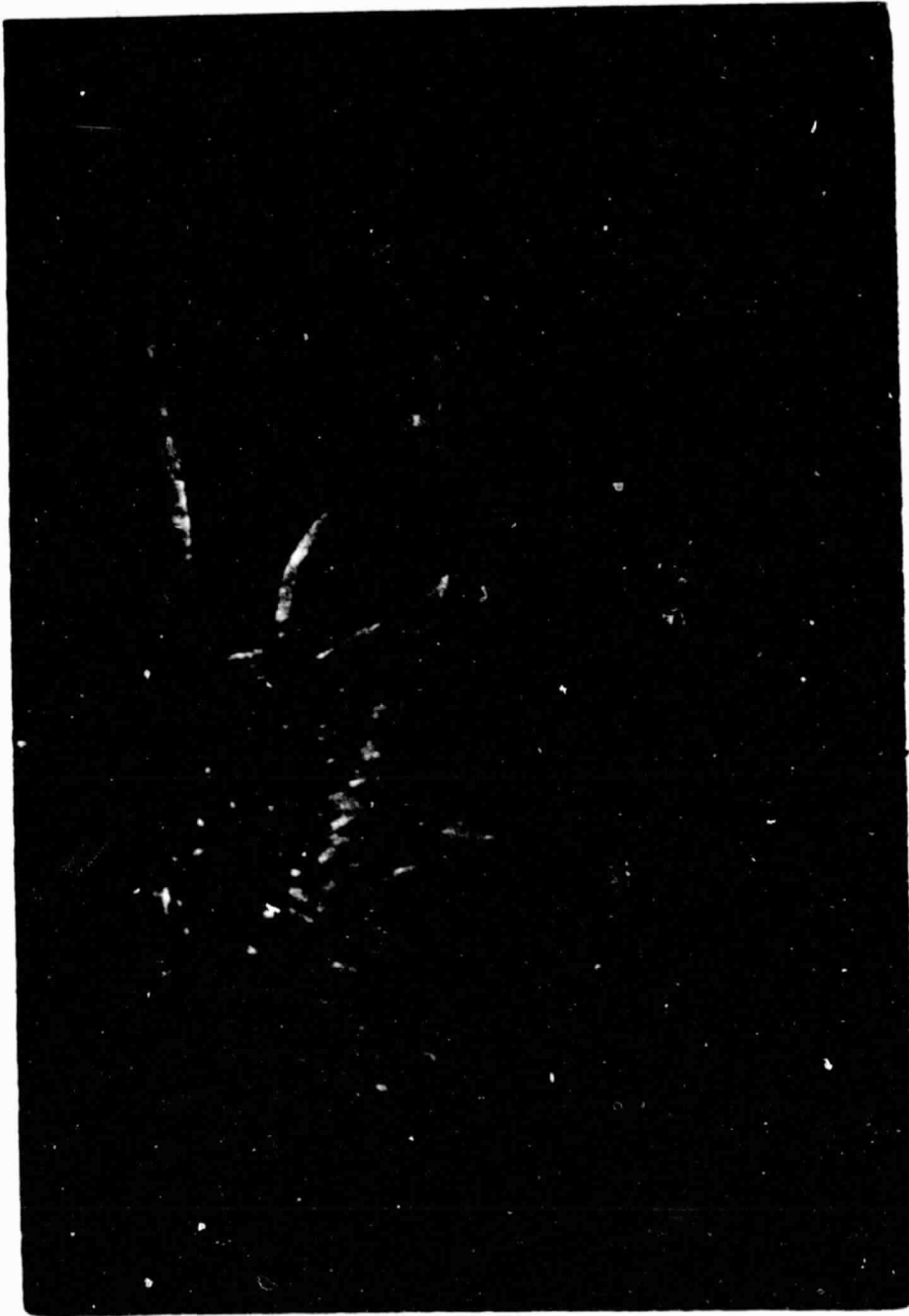


Figure 10. Photograph Showing Low Visibility of Coal Dust Even
at the Shearing Drum.

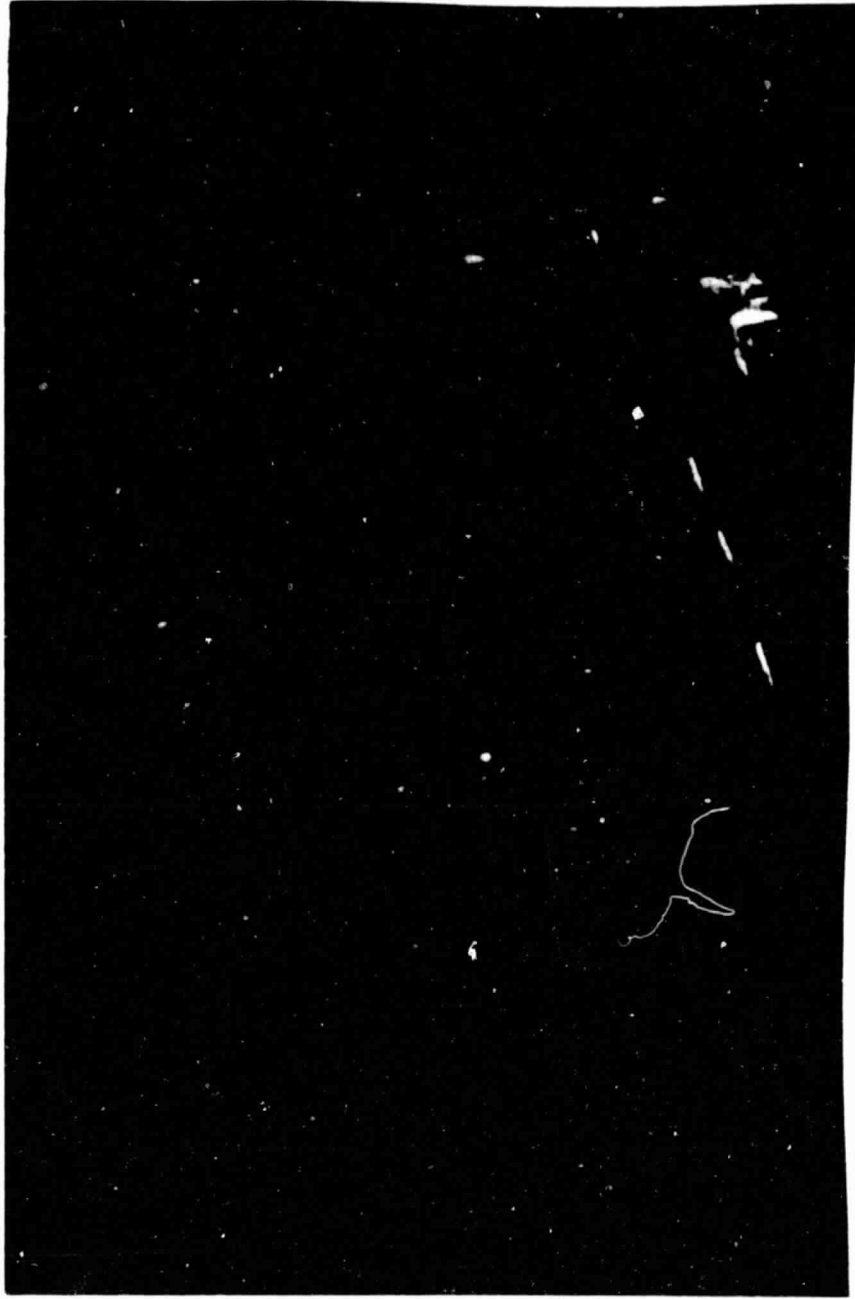


Figure 11. Photograph Showing the High Visibility of Water Jets Even at Considerable Distance.

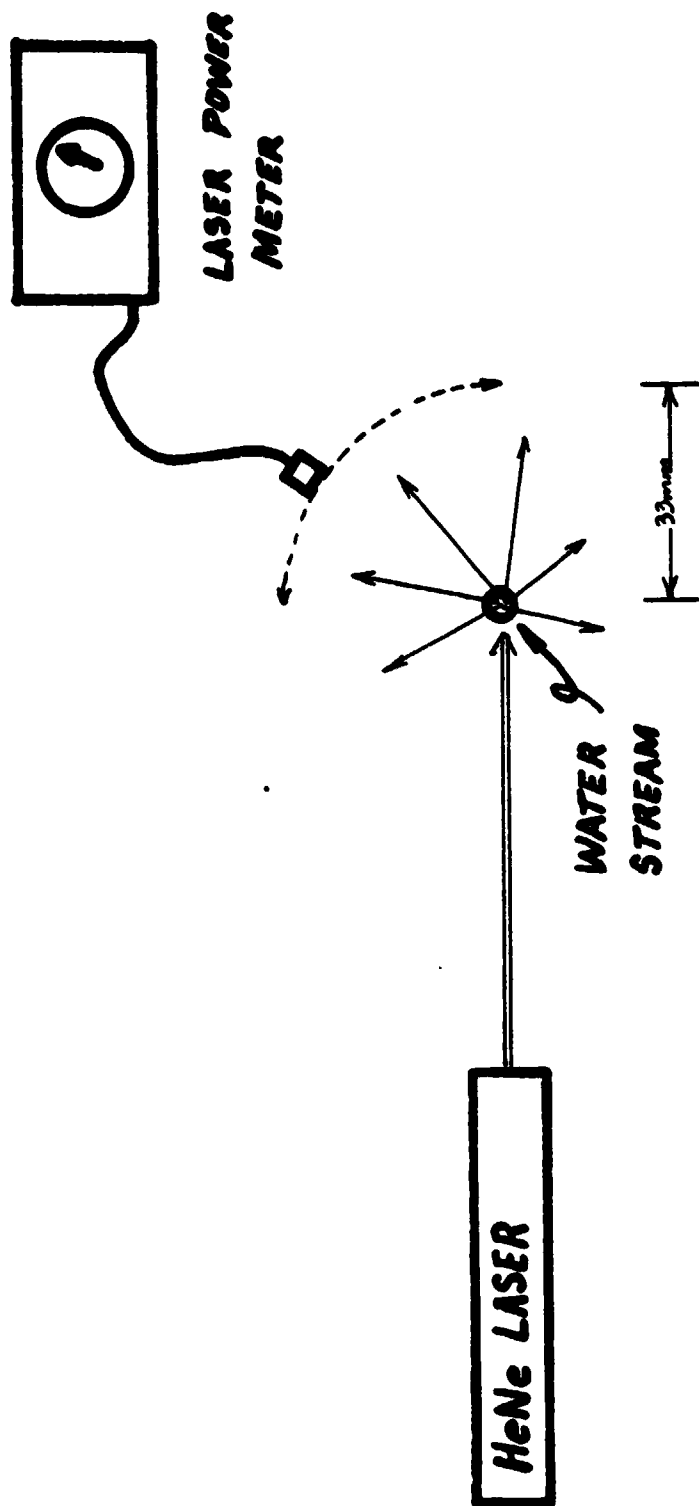


Figure 12. Schematic of Arrangement for Water Stream Measurements.

with a circular silicon sensor with 1 cm^2 area. As the plots of Figure 13 show, the smaller the diameter of the water stream the more laser light is deflected from the axis to the sides. This wider pattern becomes somewhat fixed when the stream diameter becomes about five times the beam diameter. This appeared to be principally the result of surface ripple.

A two millimeter diameter flow was examined in two forms. The first form was a smooth flowing column-like stream. This vertical stream spread the light in the horizontal plane much as a thin glass rod would. In effect, it acted like a cylindrical lens. With the photodetector placed 33mm from the stream the horizontal spreading was over tens of degrees. The vertical spreading was only enough to expand the beam to approximately 2mm.

The second form of the 2mm water stream was turbulent flow. This examination was made by simply looking at the smooth stream at a lower point along its fall, where cohesive forces tended to begin spherical formation. In this case the light was dispersed more two dimensionally. This dispersion appeared axially symmetric to the beam for all visual purposes. Most of the laser energy seemed to be unaltered. This was determined by making on-axis measurements with and without the water flow in the beam. Measured powers were 1.1mw and 1.8mw, respectively. This corresponds to a 40% scattering figure. Allowing that an entire target volume can be filled with water droplets (an impossibility for coal dust) the use of water as target material will provide a signal over a million times stronger than that expected from coal. For example, the measured value 45°

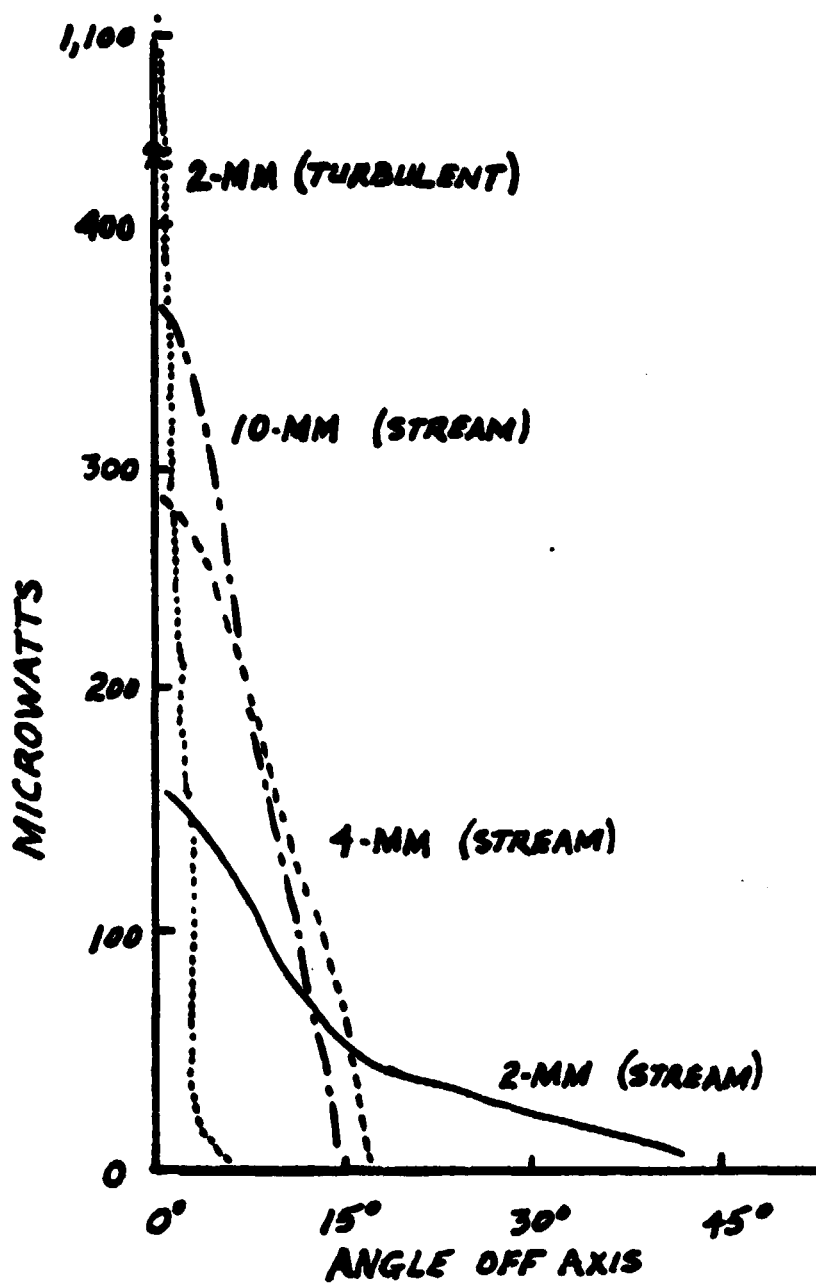


Figure 13. Results of Water Stream Measurements.

off axis is 60nW/cm^2 at 33mm distance. Calculations in Section 2.4.1 suggest irradiances of $1 \times 10^6\text{nW}$ can be expected for coal dust.

The isotropic nature of the water droplet scattering is very important. Otherwise, the sensor would have to be in a narrow scattering plane. This would greatly impede practical implementation for several reason, including the fact that the laser beams may not all lie in the same plane, that the sensor locations may be vulnerable to damage and that the plane of the laser is unknown (that is the purpose of the measurement).

Turbulant flow was not produced with the 4mm and 10mm water streams. Measurements of the smoothly flowing stream showed the cylindrical lens analogy remained reasonably valid. However, the vertical deflection was considerable more marked than in the 2mm stream.

The idea of imposing (and perhaps even scanning) streams of water droplets provides an entirely new potential. This will be exploited in later design discussions.

The difference between water droplets as would be used in the coal mine system and water droplets found in weather clouds is worth noting. In the case of the coal mine water droplets the efficiency of beam scatter is related to the ratio of laser beam diameter to droplet size. In the case of clouds, the scattering is modeled by the ratio of laser beam wavelength to droplet size. The droplets in the just described experiments were on the millimeter order, as was the beam diameter. For clouds the wavelength would be

on the order of a micrometer, with the droplets typically between 1mm and 10mm. In the first case we measured about 40% scatter. For clouds a typical albedo might be 70%. Accordingly, it is seen that no extreme benefit is afforded by creating a mist rather than droplets. On the other hand, severe disadvantages are encountered. Droplets are easier to form and their trajectories are not so easily deviated by air currents. These factors would play a significant role.

2.1.5.2 Photographic Measurements

A 35mm camera was used in the arrangement shown in Figure 14. A helium neon laser beam was projected unobscured in a darkened area. The laser light was not visible to the camera because no scattering agent was within the field of view. The camera shutter was opened for a time exposure and the jet from a commercial Water Pik^R was passed transversely through the field of view. When the water jet intersected the beam, the location of that event was readily recorded.

Observations were made with the laser only a few meters from the camera and water jet. The water stream nozzle was within a meter of the beam. A second set of observations was made with the laser traveling approximately 100 meters and the water jet nozzle located about three (3) meters away from the beam. The photographic prints shown in Figure 15 illustrate the clear detectability in both cases.

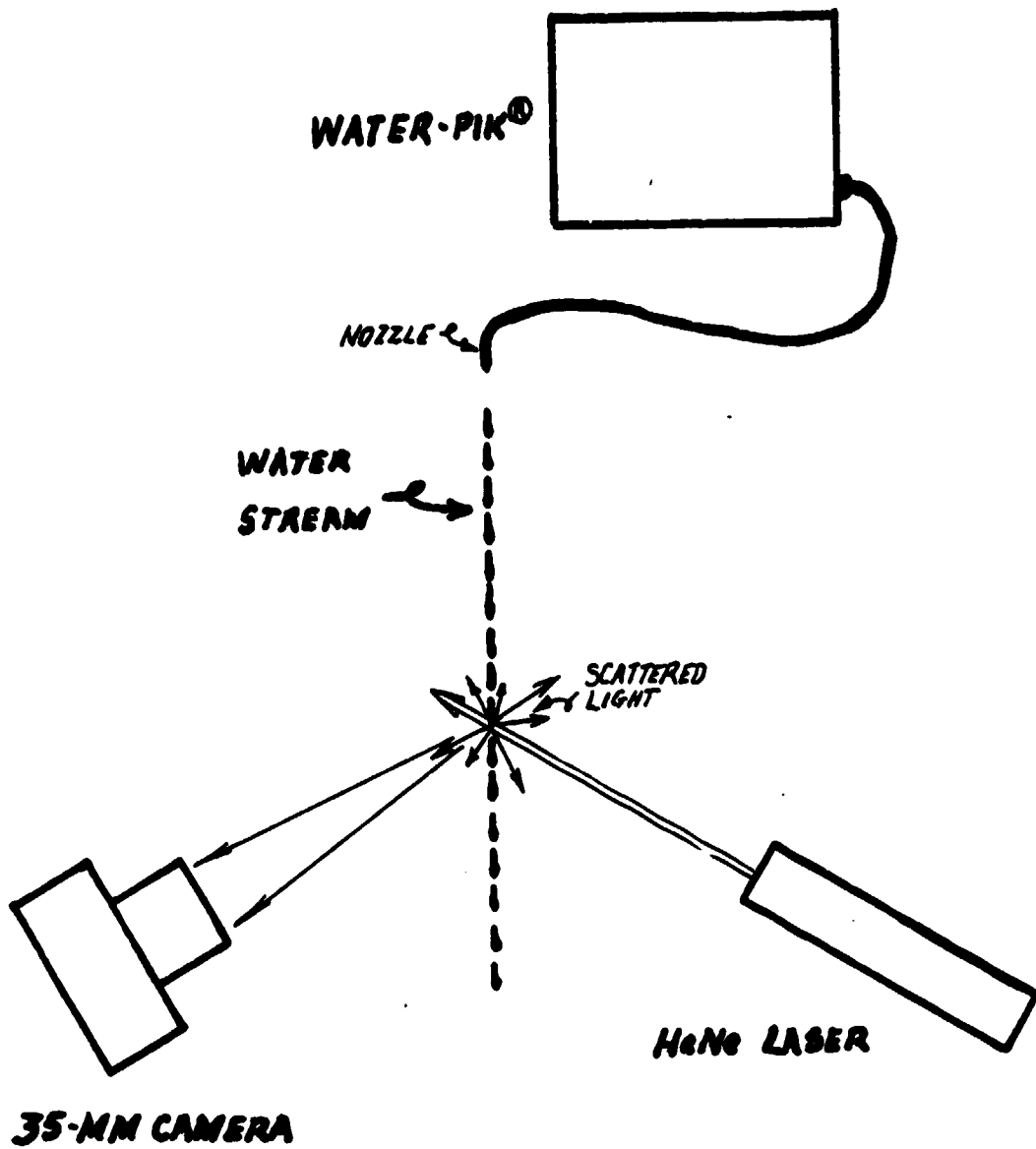


Figure 14. Arrangement for Photographic Tests.

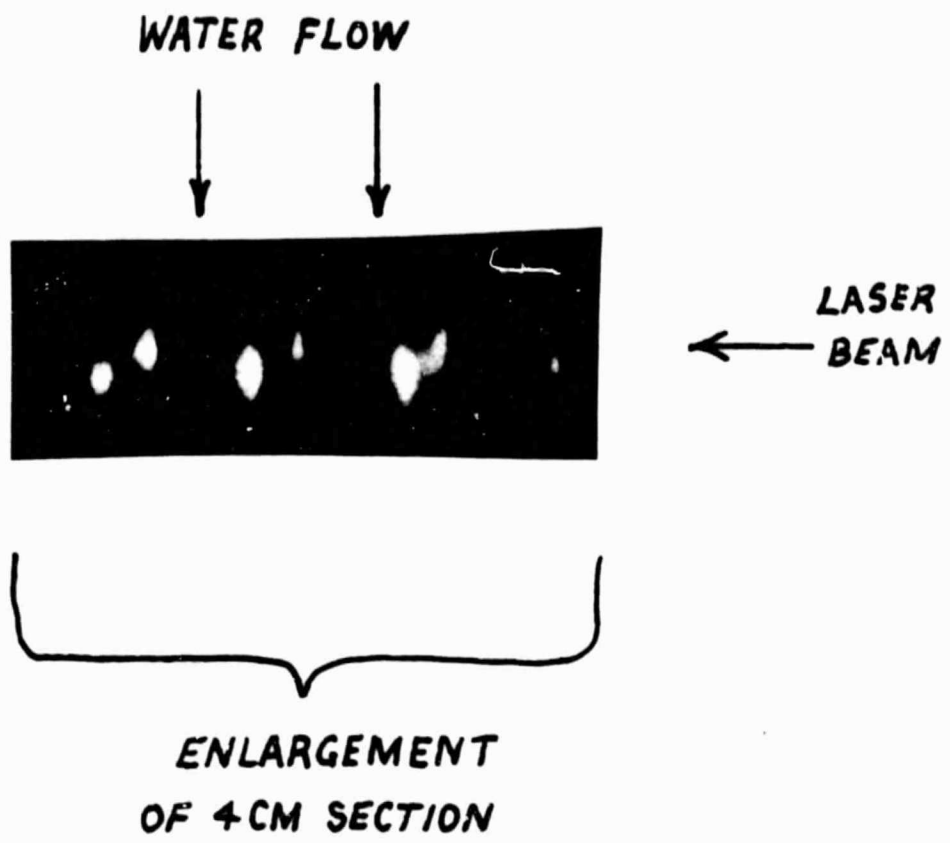


Figure 15. Example Photographic Results.

2.2 INTERVENING MEDIUM

The intervening medium is significant because it can create dispersions of the light which reduce both the signal strength as seen by the detector and the discernible spatial extent of the target. The first problem results from spectral attenuation. The second from degrading MTF (modulation transfer function). Both are subject to "micrometeorology" and scintillation.

The analysis of Section 2.1.3 and 2.1.4 divided the intervening medium between the laser source at the region near the shearer into two categories. One category included various large sized projectiles following a trajectory between the region of mechanical shear and the surrounding lower level along a course defined by gravity and initially imparted kinetic energy. This category was found to be ignorable. The second category considered suspended particles. The second category is of concern.

Assuming the distribution of suspended particles to be that of Figure 9 in Section 2.1.3, the fraction of light passing through a length of one meter can be computed. The cross section of the average particle in suspension is $9.7 \times 10^{-6} \text{ cm}^{-2}$. This assumes that particles are not masked by one another. Such an assumption is quite reasonable based on the relative values of the various numbers.

The fraction of non-scattered light exiting the one meter column compared with the light entering the column will be very nearly 100%:

$$\frac{1.00 - 9.7 \times 10^{-4}}{1.00} \approx 1.00$$

This corresponds to an attenuation coefficient of $9.7 \times 10^{-4} \text{ m}^{-1}$.

The total extinction coefficient β_{ex} is the sum of the scattering and absorption elements. Therefore, the case at hand has

$$\beta_{\text{ex}} = 9.7 \times 10^{-4} \text{ m}^{-1}.$$

This coefficient is used in the standard exponential equation for optical extinction which relates incident energy I_0 to output energy I as the pathlength of propagation X is varied,

$$I = I_0 \exp(-\beta_{\text{ex}} X).$$

This relationship shows that about 86% of the light would make its way uninterrupted down a 500 foot tunnel having the maximum respirable particle density allowed by law. Even if the factors assumed in the analysis were collectively off by a factor of five, approximately 47% of the light would still make its way down the tunnel.

For the numbers calculated, beam collimation degradation will be dominated by laser divergence. The contribution from scattering by intervening medium will contribute negligibly to the degradation for the limited fields of observation associated with any of the contemplated designs.

2.3 ILLUMINATORS

Low power lasers are used as illuminators in all the design options. Two candidates are available. One is the helium-neon laser. The other is the charge-injection gallium arsenide laser.

Choice between the two must be based on the spectral and temporal outputs, as well as the control optics which steer the beam and provide for minimal beam divergence. Furthermore, eye safety considerations and power supply requirements must be accounted for.

Figures 16 and 17 show typical construction principles and operating specifications for the two candidate laser types. From a spectral standpoint it is significant to note that the 0.85um wavelength is favored for detection with silicon photosensors. From a safety standpoint, tabulated values of accessible emission limits for laser products indicate for Class I CW operation with no scanning and 1-second integration time that only 0.7mw is allowed at 0.63um, while 1.4mw are allowed at 0.85um. Therefore, the gallium arsenide laser would seem to be favored by both detection and safety factors. However, since this laser is not visible to the human eye the potential operational advantages of visually seeing the beam are lost.

Calculations which follow show that neither the 0.7mw nor the 1.4mw levels are suitable to detection using the coal or water scattering approaches. Greater power is needed for reliable operation. It should be noted that a scanned laser, with failure guard, would allow a great increase in power output.

The power supply requirements favor the use of gallium arsenide because it is low voltage and displays low current drain. Ruggedness, temporal control and small size also favor this candidate. Nevertheless, calculated trades must be undertaken on an overall basis before selections can be recommended.

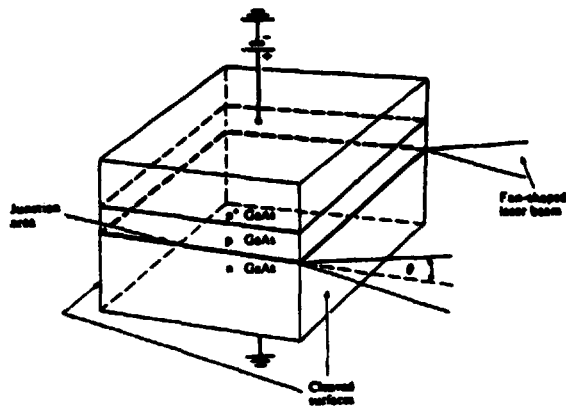


Figure 16. Schematic construction of gallium arsenide laser. Typical parameter include: wavelength of 0.85 μm , operates on less than 3 vdc, 200 ma, size less than 1 cubic inch.

ORIGINAL PAGE IS
OF POOR QUALITY

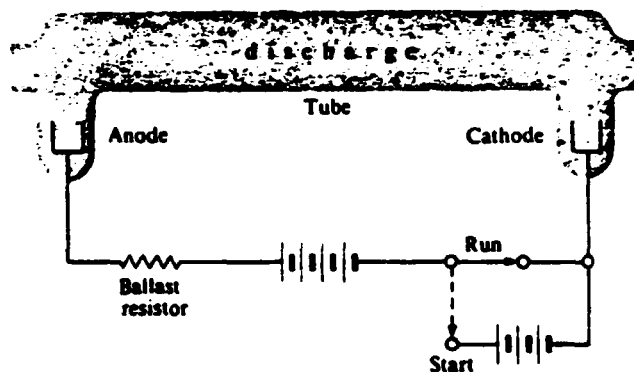


Figure 17. Schematic construction of helium neon laser. Typical parameters of 0.63 μm , operates at several hundred volts, size greater than 50 cubic inches.

AS

2.4 TRADE CALCULATIONS

This section will establish the reasonable bounds for the use of laser beams, scattered from coal particles and from water, as references for instantaneous longwall shearer location. The sensor system used for these trade considerations assumes certain ideal characteristics which will become apparent throughout the discussion.

2.4.1 Available Light From Coal Dust

In this subsection we will examine how much light is available for detection. This will start by assuming a laser output and addressing the question: How much light is scattered by a single "average particle"?

Assume a 1mw laser beam over a 1cm^2 diameter, if the particle does not absorb, the scattered power is

$$(1 \text{ mw}) \left(\frac{9.73 \times 10^{-6} \text{ cm}^2}{1 \text{ cm}^2} \right) = 9.73 \times 10^{-6} \text{ mw}$$
$$= 9.73 \times 10^{-9} \text{ W per particle}$$

Assume we collect this with a 10cm^2 aperture at 1 meter to the side, with particle reflection of roughly 1×10^{-4} and scattering evenly distributed over 4π steradians. The power collected by the aperture will be

$$\left(\frac{10\text{cm}^2}{10^4 \text{cm}^2} \right) (1 \times 10^{-4}) (9.7 \times 10^{-9} \text{ W}) = \frac{9.7 \times 10^{-16}}{4 \pi}$$
$$P_{\text{particle}} = 7.7 \times 10^{-17} \text{ Watts}$$

If we assume 100% optical efficiency and a detector NEP of 100 pw at 1 KHz sampling frequency, we can calculate the number density needed for detection:

$$\frac{(100 \times 10^{-12} \text{ W})}{7.7 \times 10^{-17} \text{ W}} = 13 \times 10^5 \text{ particles}$$

If we change to a sampling frequency of 10 Hz we have

$13 \times 10^5 \sqrt{\frac{10}{1000}} = 13 \times 10^4 \text{ particles/cm}^3$ in our field view is limited to 1 cm^2 . If we look lengthwise along the beam for 10cm, the number density becomes

$$1.3 \times 10^4 \text{ particles/cm}^3 \text{ for detection}$$

The 1×10^{-4} assumption for reflection coefficient may be too conservative. Adjunct Systems measurements, as well as published data, suggest 0.03 to 0.15 is likely. The factor of 30 to 150 over the assumption gives a needed density between 90 and 430 particles/cm³. Therefore, let's use a rule of thumb for now that detection unity signal-to-noise ratio requires 100 particles/cm³. This is a thousand times the MSHA allowance.

2.4.2 Available Light from Water Stream

The water stream can be designed to completely intersect the laser beam. This gives a cross section tens of millions of times that of 100 coal particles of 10um diameter. Additionally, the absorption of the water droplets is typically ten times less than coal. A 1-milliwatt beam scattered isotropically by the water could provide better than 10 microwatts of radiant power on the detector

using the optics of the previous section. Signals of this level would allow use of large area detectors with rapid sampling. The advantage of a large area detector is allowance of large angle fields of view to minimize scanning the sensor.

2.5 IN-MINE EXPERIMENTAL APPARATUS

The key test associated with the original shearer location concept is concerned with the visibility of the beam as scattered by the coal dust particles and the degree of attenuation encountered by the reference beams. An apparatus was designed to conduct in-mine experiments to ascertain such visibility and attenuation. The experimental apparatus has been designed to avoid delays of manufacture and certification. At the same time, the apparatus provides for unambiguous determination of concept viability.

A standard miner's lamp was mounted against a plastic diffusion screen which was fastened onto the side of a 1x1x1 foot metal case, as illustrated in figure 18. A second diffusing plate was positioned across from the first to provide a 1-ft square source of doubly-diffused light. By experimentation, it was determined that the variation in intensity over the camera resolved region would be less than 5%.

A 35-mm camera was equipped with a 450-mm telephoto lens. This lens fills the camera frame at 60-ft to the extent that it may be considered an extended source. By placing a matrix of differing neutral density filters near the image plane of the camera, the density versus exposure calibration can be made from a single frame of film. Figure 19 shows the camera arrangement. It allows easy

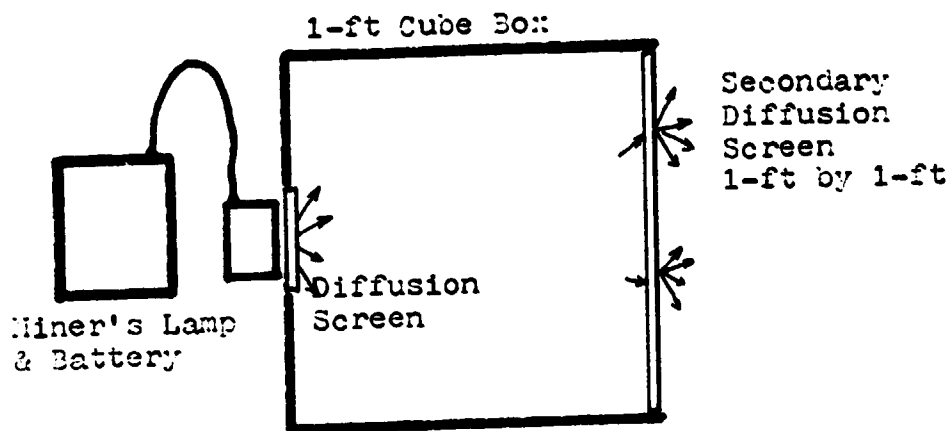


Figure 18. Light Source Arrangement for Mine Tests.

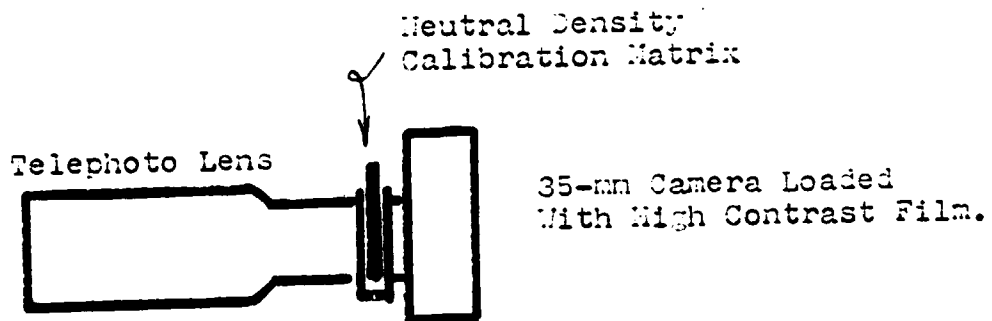


Figure 19. Camera Arrangement for Mine Tests.

insertion and removal of the calibration matrix.

High contrast film was used in the experiment depicted in Figure 20. This maximized sensitivity to changes in recorded intensity that might result from attenuation by coal dust. No change was noted between the presense and absense of the shearing machine alongside (or in between) the camera and light source arrangement. Estimated sensitivity was 10% or better.

AS

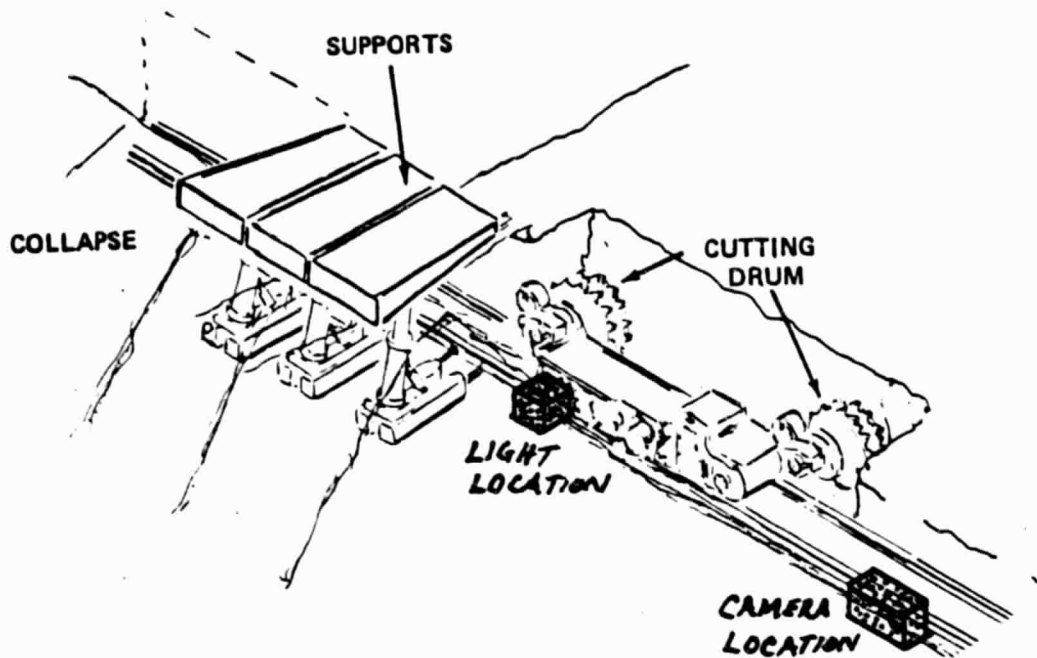


Figure 20. In-Mine Photographic Measurement Set-Up. The Diffuse Light Source Was Positioned Approximately 60-ft from the Camera as the Shearer Passed Alongside.

ORIGINAL PAGE IS
OF POOR QUALITY

AS

3. SENSOR SYSTEM OPTIONS

(TASK #2)

The results of Task 1 as related in the previous section are used here to determine what sensor system characteristics are needed to observe laser beams as scattered from coal dust or water, along the longwall operation. Consideration is given to blocks #2, #3 and #5 through #11 of Figure 4 in the Introduction.

3.1 BACKGROUND

Generally speaking, the eletro-optical background to be seen by the sensor is favorable because of the tunnel's darkened condition. Some concern must be given, however, to the possibility that some tunnels may be fitted with lights or, at minimum, the miner's head lamps will cross the sensor field of view from time to time. Such possibilities can be overcome by rejecting them with optical analyzers on the basis of spectral, spatial and temporal features.

An appropriate bandpass filter is recommended for use with either the gallium arsenide or the helium neon laser. This bandpass filter would be placed immediately in front of the photodetector in the sensor system. All but the laser wavelength would be rejected.

3.2 INTERVENING MEDIUM

If the number density of particles between the reference beam

and the sensor aperture is high, then the possibility exists that an otherwise adequate laser scatter would be obscured. The positioning of sensors on the shearer body must take in account such a potential. The physical relationships for this signal attenuation are the same as detailed in Section 2.

The case of beam propagation down the longwall tunnel showed suspended particle and small projectiles to be the main contributors to beam attenuation. This circumstance was the consequence of the beams being significantly distant from the shearer region path of direct trajectory. The sensor, by contrast, is located much closer to this path. However, the photographic analysis discussed earlier showed neither major advantage nor disadvantage for this circumstance.

3.3 OPTICS

The aperture of the optics is restricted by several practical considerations. Not least among these are MSHA requirements on windows in explosion proof housing. Nevertheless, such requirements are not the governing factor. The prevailing thought is to use an off-the-shelf collector with short enough focal length for small system packaging and the use of small photodetectors. The small package advantage is self evident. The value of the small detector is minimization of detector inherent noises. These noises increase approximately with the square root of the detector area. For a given target size (reference beam segment), the size of the

image will increase with optical focal length. Accordingly, the smaller focal length will decrease the detector dimensions.

The possibility exists for using a single element collector lens in both the coal dust scatter and the water scatter concepts. Typical camera lenses have multiple elements. One purpose of the multiple lens element design is to reduce chromatic aberration. That is, to eliminate the multiple focal lengths which characterize a simple, single element lens, the cause of colorized blurring. Because the laser light is monochromatic, chromatic aberration would not be a problem. However, other aberrations would still exist. Use of lenses having aspheric shapes can help somewhat in this regard. It turns out, however, that it is more difficult to obtain a required aspheric than to procure a standard camera lens having the added advantages of field flatness and aperture control. Therefore, lens type selection must await more detailed investigation of a specific design. For now, a commercial camera lens is assumed.

Packaging and detector sizing suggest a lens with a 35mm to 75mm focal length for either approach. Signal strength requirements push to f-numbers between $f/2$ and $f/1.4$ for coal dust, with $f/5.6$ adequate for water. Availability suggests use of 35mm photographic camera lenses or video camera lenses. These have been designed for excellent performance with regard to image plane flatness over a large field of view, with baffling suitable to conditions of direct sunlight striking the lens system obliquely. The second factor also means commercial camera lenses are designed with very low scattering coefficients.

3.4 ANALYZERS

The use of spectral bandpass filters has already been discussed. Other analyzers have limited value. Polarizers would only serve in this case to reduce signal-to-noise in the system by cutting down the scattered light level. Since the lasers are monochromatic, gratings and prisms are inappropriate.

3.5 TARGET SCAN

Target scan options are extremely important to the design of the shearer locating sensor. The trade between total and instantaneous field of view with scan rates and times is a major system parameter driver. This is principally because the dwell time of the reference beam image of the detector should be as long as possible to maximize the system operational signal-to-noise ratio and the detection threshold.

The coal dust target approach requires the use of small detectors. This means an array of detectors and complex scanning in order to obtain needed dwell. The water target concept has sufficient signal-to-noise to combine a relatively large field of view in the sensor as a whole with an artificial instantaneous field of view derived by sweeping the target water stream instead of the sensor. This minimizes the number of detectors required and avoids sophisticated focal plane scanning. Long dwell times are achieved as long as background contributions are low.

The third approach, angular swept laser beams, has signal-to-noise ratios even far greater than the water target approach. This allows use of staring (non-scanned) optics and detector with little concern over background.

3.6 BACKGROUND SCAN

The sensor configuration must regard scanning of the background. The concept using suspended coal dust to make visible reference laser beams, as shown in Figure 2, operates with a small instantaneous field of view (IFOV) matched spatially to the expected beam appearance. This IFOV is scanned within the sensor's total field of view (TFOV) to derive angular location of the beam with respect to a shearer body reference.

The same particles of coal which provide the laser beam target can scatter light from a miner's lamp or other mine illumination. The use of a narrow spectral bandpass filter will keep contributions from this background source to levels of the same order as the laser signal. The headlamp contributions would be intermittent and random. As such, they can be rejected by system logic.

Steady illumination sources in the mine will not provide the same competition that a headlamp will. The steady illumination arising within the sensor spectral passband will appear as an extended source. Accordingly, as it is scanned by the sensor IFOV, its major effect will be to increase the d.c. signal level. This d.c. component is easily filtered by capacitance coupling in the

electronics. Nevertheless, the random nature of the background distributions will provide some component within the sensor's temporal frequency passband, adding to system noise.

Steady illumination is a more serious problem for the sensor if it provides glint from the coal mine walls and from mining equipment (e.g. support chocks). The scanning of this glint, even with optical spectral filtering, will very much compete with the low level laser signals in the coal dust scatter approach. The effective scattering cross sections of the solid objects will be tens of thousands of times greater than that of suspended dust. Bulk filtering to extract the meaningful signals must be required. Kalman filtering techniques would be applicable here, but might necessitate considerable computer power.

The concept using an imposed water plane, illustrated in Figure 3, is subject to the same background considerations of the coal dust concept but with less severity. The principle difference is that the target cross sections can be as big as the glint cross sections and that the water plane can be steady enough to allow a carrier frequency on the laser beam to facilitate frequency rejection of the background.

3.7 DETECTORS

The radiance of the laser is I watts/steradian. The solid angle within which the radiance is contained is ω steradians. For simplicity in calculation the assumption will be made that the substance

of beam is of square shape. This leads to a square beam of dimension $\sqrt{\omega} \times \sqrt{\omega}$ for either concept. Reference to the Fraunhofer photographs of the gallium arsenide laser which were made in the laboratory suggests that the assumption of the square beam is not particularly less accurate than assumption of a beam with circular cross section.

3.7.1 Detector Size

The distance from the source to the point where the beam crosses the sensor's instantaneous field of view (IFOV) in the coal dust case is symbolized by D. For the case at hand, the IFOV is defined by the dimensions of the photodetector and the length from the principle plane of the collecting optics to the detector plane, designated by l_d . A square photodetector is typical for commercially available devices. Design practice is to match the detector size to the anticipated target image size. If the detector is smaller than the image some of the available signal will be lost. If the detector is larger the system will have unnecessarily sacrificed spatial resolution as well as have increased detector noise, which increases as the square root of detector area.

The length l_d is related to the distance between the target region and the sensor l_t , through the lens focal length f. The simple thin lens equation is adequate for the accuracies required here. This is expressed as

$$\frac{1}{l_d} + \frac{1}{l_t} = \frac{1}{f}$$

The values of l_d and l_t also enter the matching of detector and target image size. A target of height H and width W will be imaged proportionate to the scaling factor:

$$\text{Scaling factor} = l_d/l_t$$

The earlier assumption of a square target leads to a spatially matched detector of sides

$$s = D \sqrt{\omega} (l_d/l_t)$$

3.7.2 Irradiance at Detector

The amount of light traversing the tunnel for a distance D is estimated from the relationship for the effective radiance of the target region

$$N = I \omega R \exp(-\beta_D D) \text{ Watts/ster}$$

Here, the laser source output I expands according to the divergence parameter ω to be reflected by the volume of airborne particles having a cumulative reflectance of R per unit solid angle. The exponential factor is simply the extinction for a coefficient β_D .

Values of R and β_D for various circumstances were provided in Section 2. Example values will be used in later calculations. They are not needed at this time as mathematical development continues for the generalized case.

Only a portion of the power N will be intercepted by the collecting optics of the sensor. This will be in accordance with the solid angle subtended by the collector, which has an area

related to the opening diameter,

$$A = \pi d^2/4.$$

This corresponds to a solid angle

$$\begin{aligned}\Omega &= A/l_t^2 \\ &= \pi d^2/4l_t^2 \text{ steradians}\end{aligned}$$

Allowing the transmission efficiency of the optics to be represented by K , the power of the light focussed onto a spatially matched detector is, after adjustment for extention between the target and collector,

$$\begin{aligned}P &= N\lambda K \exp(-\beta_t l_t) \\ &= I R K \exp(-(\beta_D D + \beta_t l_t)) \\ &= \frac{I \omega R \Omega d^2 k}{4l_t^2} \exp(-(\beta_D D + \beta_t l_t)) \text{ Watts}\end{aligned}$$

The relationship developed earlier for the detector dimension can be recast into the form

$$l_t = D \sqrt{\omega} (l_d/s)$$

Substitution into the equation for P yields, for the case $f=l_d$

$$P = \frac{I R \pi K s^2 \exp(-(\beta_D D + \beta_t l_t))}{4D^2 F^2}$$

Where F is the lens F -number, f/d . The assumption that $f = l_d$ arrives from $l_t \gg l_d$, as is reasonable for geometrical considerations of the coal mine implementation.

3.7.3 Detection Signal-To-Noise Ratio

The performance of detector devices is often given in terms of irradiant power needed to produce an electrical effect equal to

the inherent detector electrical noises. Normalized for area, a , and electrical bandwidth Δf , the reciprocal of this noise equivalent power (NEP) is often stated as specific detectivity.

$$D^* = \frac{\sqrt{a \Delta f}}{\text{NEP}} \quad \frac{\text{cm} \sqrt{\text{Hz}}}{\text{W}}$$

However, in the case of fluctuations in the light due to coal mine particles, this might not be appropriate. The scintillations of the particles may cause noise effects much larger than the inherent detector noise. The level of scintillation can be estimated to a first order by taking the square root of the number of target particles and using it in the power equation. This estimate is based upon the assumption of equally sized, randomly distributed isotropic scattering particles contained in the laser beam scattering region being viewed by the sensor.

Additional scintillation is produced by distribution differences in particles along the path D and the path l_t . Nevertheless, the values shown in the figure illustrate the idea that the noise may originate more from target parameters than electronics performances.

All sensor optics, whether based on gallium-arsenide or helium-neon lasers, will use silicon photodetectors. Figure 21 through 23 indicate representative performances for commercially available devices. These will be used in later Sections for tradeoff calculations. The type designations are those used in the Handbook of Optics. The data shown are for Type I and Type IV devices.

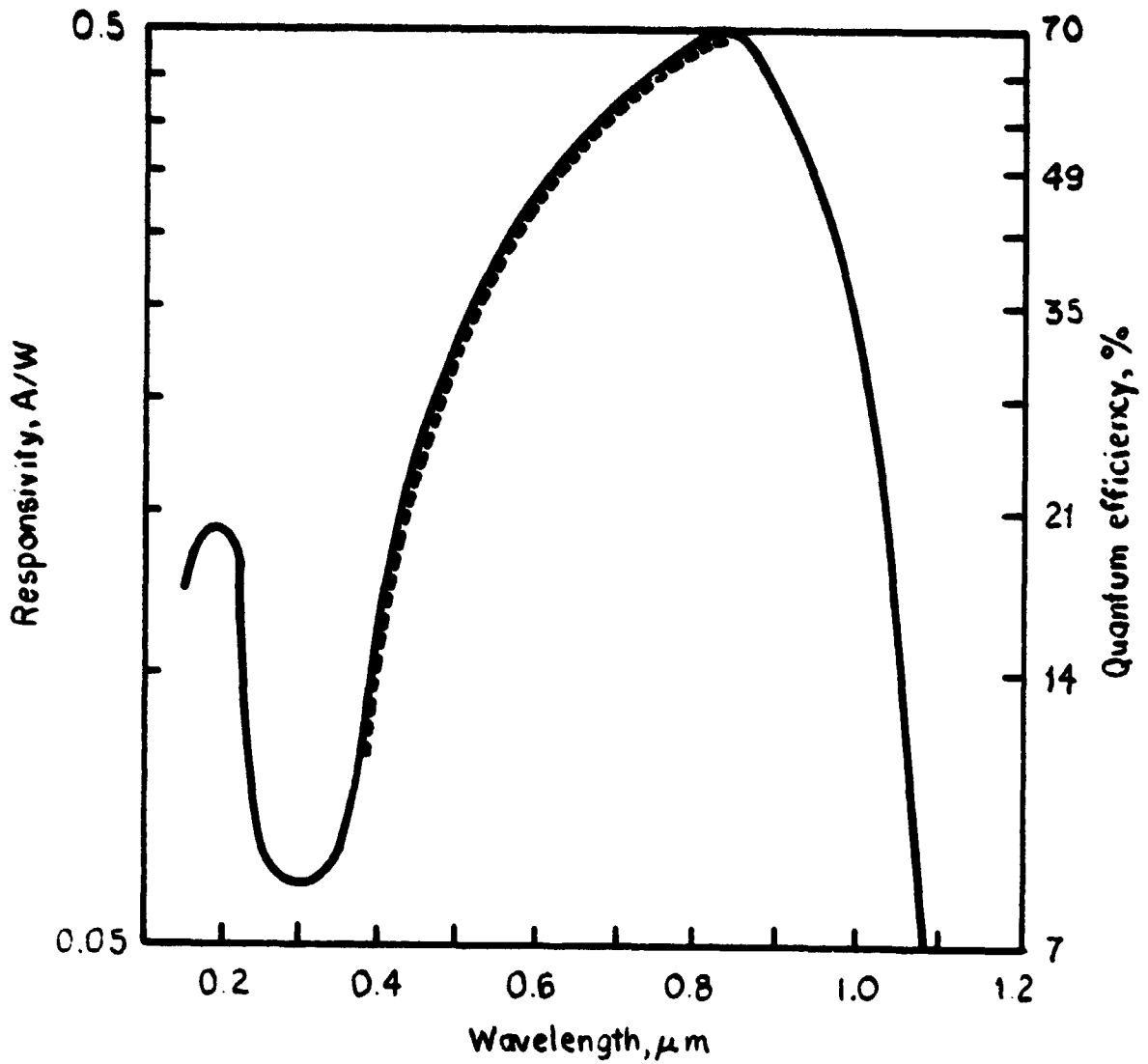


Figure 21. Spectral Curves for Type I Silicon Detectors.

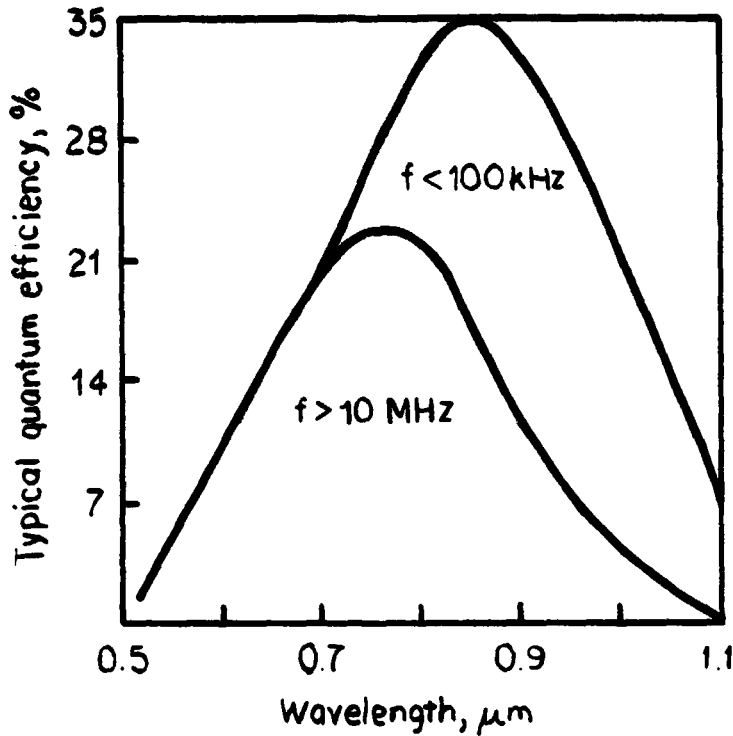


Figure 22. Typical Quantum Efficiency as a Function of Wavelength for Silicon Avalanche Photodiode at 298° K.

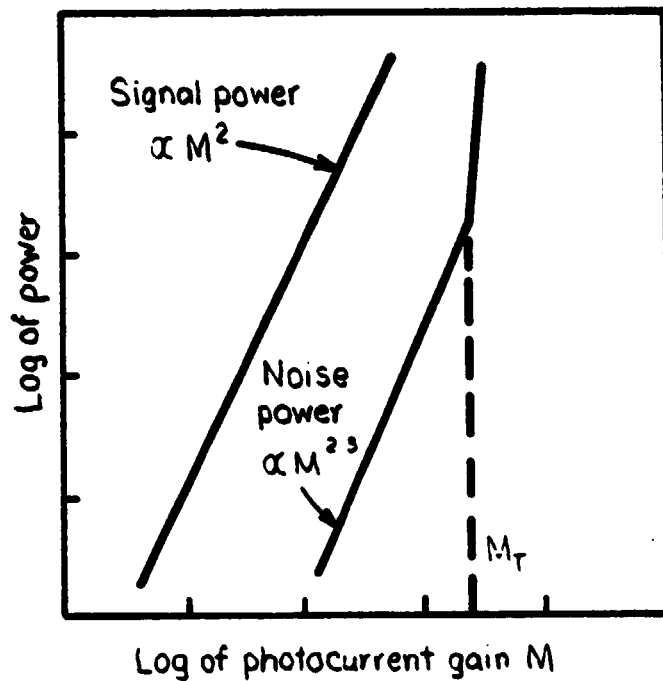


Figure 23. Signal Power and Noise Power as Functions of Photocurrent Gain for a Silicon Avalanche Photodiode.

3.7.3.1 Type I Detector

This form was historically the first to be developed. It is generally used when high sensitivity is required and time constants slower than μs are permissible (see types III and IV for modified spectral distributions).

Sensitivity: $D^*(\lambda_{pk}) \approx 10^{12}$, $D^*(2,800\text{K}) \approx 2 \times 10^4 \text{ cm Hz}^{1/2}/\text{W}$,

becoming amplifier-limited for small-area detectors.

- Noise: As T drops, impedance rises, so that decreasing noise current produces increasing noise voltage. However, the signal increases even faster, yielding an improved signal-to-noise ratio when cooling.
- Capacitance: Capacitance is proportional to area and increases slightly with temperature.
- Responsivity: See Figure.
- Quantum efficiency: 90 percent quantum efficiency achievable with antireflection coating.
- Sensitive area: 0.05 to 25mm (linear dimensions).
- Time constant: Inherently slower than IIs for high-sensitivity applications, limited by RC.
- Operating temperature: Ambient
- Recommended circuit: See Figure. High impedance FET current-mode amplifier to supply fixed bias voltage, regardless of current.
- Manufacturers: Texas Instruments, Electro-Nuclear Labs, RCA, Solar Systems, Inc., Honeywell, Mullard (Optoelectronics).

3.7.3.2 Type V Detector

The avalanche photodiode is especially useful where both fast response and high sensitivity are required. Whereas normal photodiodes become thermal-noise-limited when heavily loaded for fast response, avalanche photodiodes make use of internal multiplication, associated with reverse breakdown in the p-n junction. Stable multiplication is made possible by a guard-ring construction, which prevents surface breakdown. However, very careful bias control is essential for stable performance. An optimum gain exists below which the system is limited by receiver noise and above which shot noise dominates receiver noise and the overall noise increases faster than the signal.

In addition to fast-response applications, avalanche photodiodes are useful whenever amplifier noise is limiting, e.g. small-area arrays. Signal-to-noise ratio improvements of one to two orders of magnitude over nonavalanche case can be achieved.

- Sensitivity: $NEP \approx 0.1 \text{ pW}$ at 10 MHz; $A = 5 \times 10^{-4} \text{ cm}^2$; gain=800
- Noise: Typically 0.2 to 10 nA. As gain increases, noise increases. Optimum gain is where avalanche noise equals system noise. Thus optimum gain is a function of system noise.
- Responsivity: Depends on photocurrent gain. Gain-bandwidth product 80 GHz at 633 nm. Spectral response depends on operating frequency.
- Quantum efficiency: Typically 35 percent peak.
- Capacitance: Depends on bias and area.
- Sensitive area: 2 to 500 $\times 10^{-5} \text{ cm}^2$.

- Series resistance: Depends on area.

$A, 10^{-4} \text{cm}^2$	f, GHz	R_s, ohms
5	90	50
45	0.9	5

- Time constant: Depends on gain (gain bandwidth 80 GHz).
- Recommended circuit: Constant-current operation can be achieved by using a reference diode to sense temperature and using its output to regulate a bias voltage, which properly varies with temperature.
- Operating Temperature: 208° to 398° K.
- Manufacturers: Texas Instruments, General Electric Co., Space Technology Products, Honeywell.

Avalanche photodetection improve the prospects of the coal dust concept somewhat. Ideally implemented the number density to obtain a signal-to-noise ratio of 10 might be reduced considerably in the absence of target noise. However, the reduced number density, $100/\text{cm}^2$, is still grossly above MSHA standards.

3.8 ELECTRONICS

A typical circuit for Type I silicon photodiodes is shown in Figure 24. Type V uses a variation on this circuit with thermally controlled variable voltage bias. Figures 25 through 28 give exemplative curves for bias and frequency parameters. Data of this

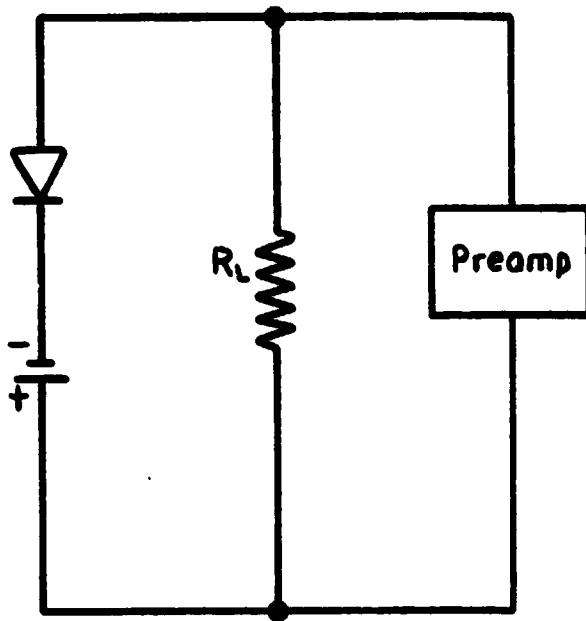


Figure 24. Recommended Circuit for Type I Photodiode.

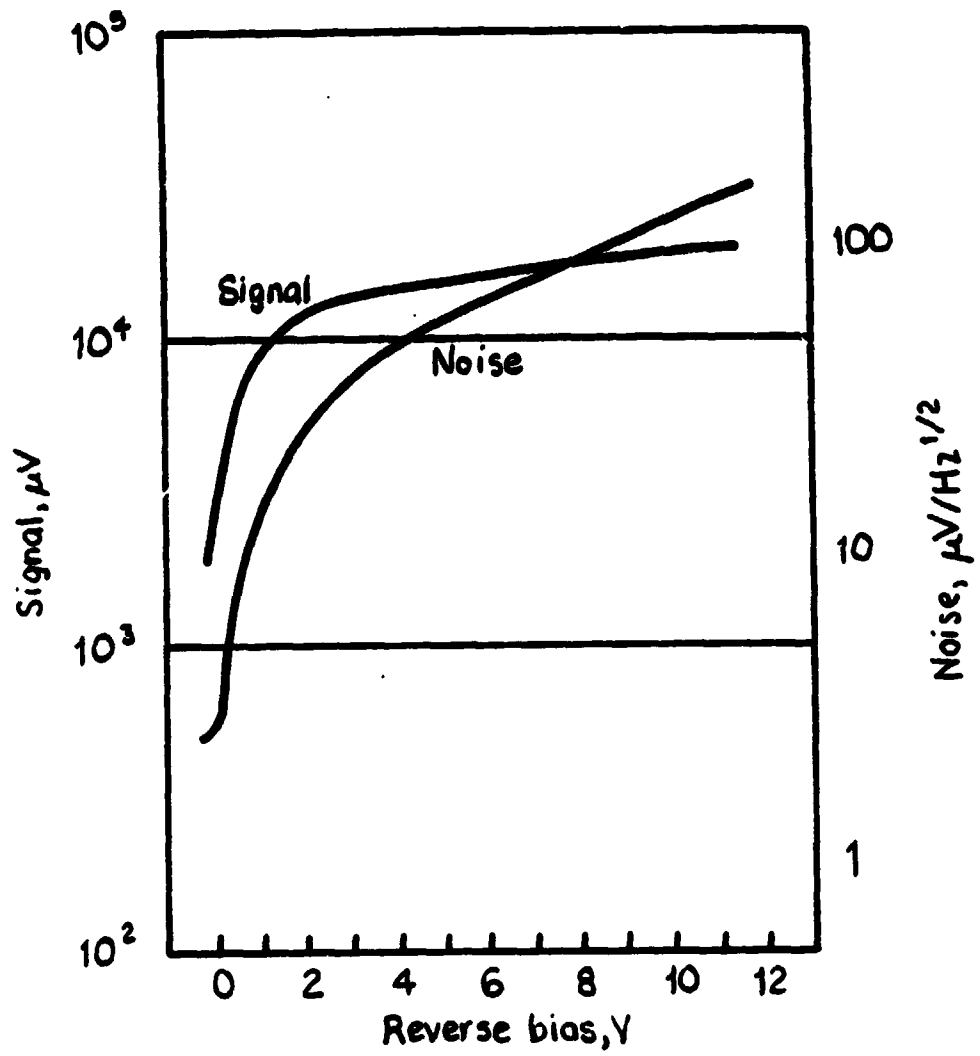


Figure 25. Typical Curve for Signal and Noise versus Reverse Bias for a Type I Photodiode with Load Resistance of 100 Megohms.

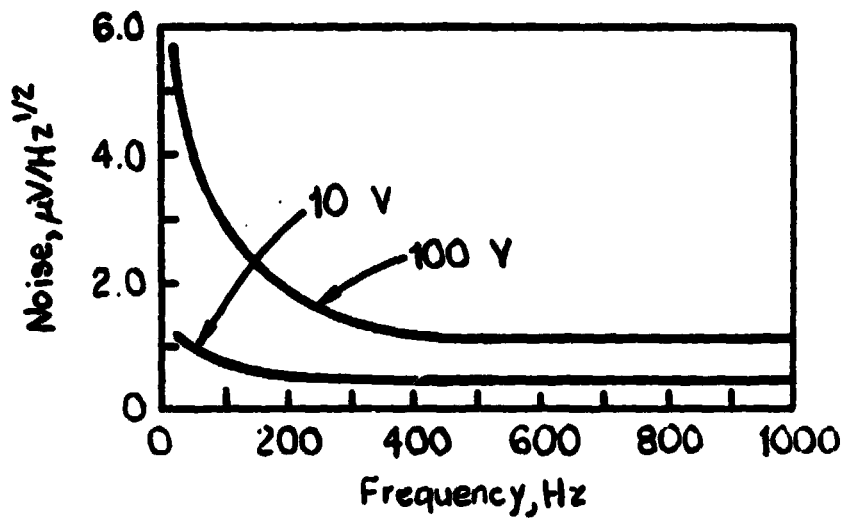


Figure 26. Typical Noise Frequency Spectrum for Type I at Different Reverse Bias; $A=1 \times 1 \text{ mm}$, and Load Resistance = 1 Megohm.

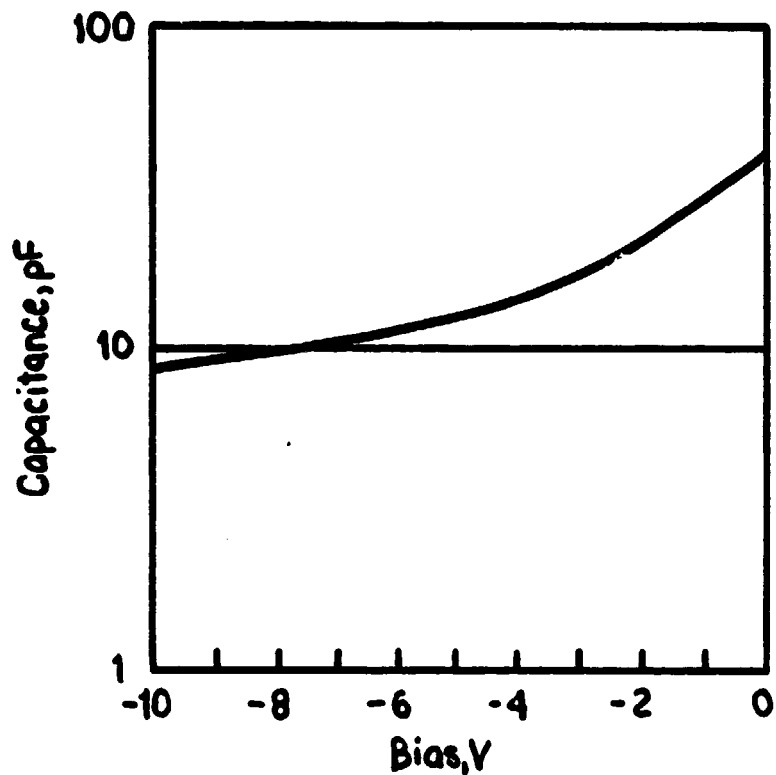


Figure 27. Capacitance as a Function of Bias for a Typical Type I Photodiode with A=2x2mm.

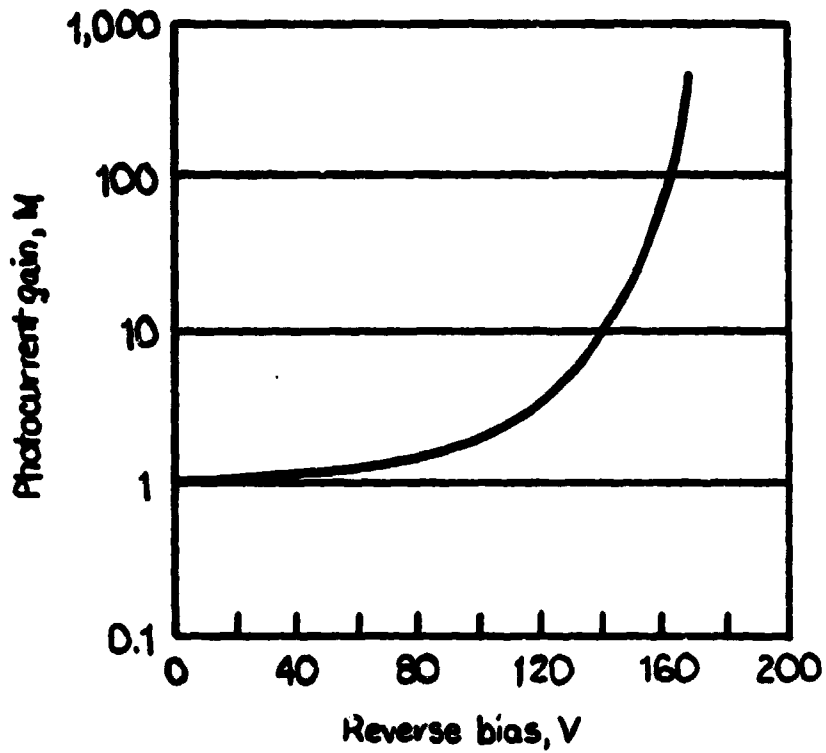


Figure 28. Photocurrent Gain as a Function of Reverse Voltage for a Type V Photodiode.

nature is readily available for most specific detectors on the commercial market.

3.9 OUTPUT DATA OPTIONS

NASA/MSFC prototyping for longwall automation thus far has utilized analog voltage outputs for parameters such as height to the last cut and for seam thickness. Analog signal output is also possible for the shearer location system. However, the spatial complexities suggest that multiple signals will have to be output. This will necessitate other multiple data lines or signal multiplexing. The state of the art in microprocessing suggests that a single digital data link might be competitive with the analog link and would allow for some degree of data processing at the sensor end of the link.

Another option, discussed later in the section on recommendations, is to link the sensors and controllers over optical channels. This eliminates the need for running cables several hundred feet along the walkways or conveyor structure.

4. SHEARER LOCATION SYSTEM

(TASKS #3 and #4)

Shearer location infers determination of the shearer in x, y and z coordinates defined as follows:

- x is the horizontal displacement when observing along the z-axis (i.e. down the longwall tunnel).
- y is the vertical displacement when observing along the z-axis (i.e. down the longwall tunnel).
- z is the distance down the longwall tunnel measured from some origin near an end.

The collect of the x, y and z coordinates as the shearer moves along the longwall defines the "trajectory" of the machinery. A key observation about this shearer trajectory is that it is completely defined by the tracks on which the machinery is propelled. A further refinement of nomenclature is the understanding that "instantaneous" location simply signifies that the determination of a set of x and y is made with resolution in z equivalent to the smallest distance in which some modification in track position is possible. In the case of a longwall operation the movement of a single roof support modifies track position. The appropriate z-axis resolution which may be considered instantaneous will be equal to, or less than, the z-axis dimension of a support element. Typically, this is five feet. Additionally, the flexibility of the track governs the highest degree of accuracy in x and y that is useful. For example, if the track can only be given a curvature of five inches per roof support, then

AS

a resolution of one inch for the location sensing system is of questionable value. This is particularly true if a great deal of added life cycle cost is incurred to obtain the high resolution.

In the following discussion, techniques for instantaneous location of the shearer are discussed from the standpoint of relevant geometries. (It is seen that positional and attitudinal (roll, pitch and yaw) measurements are interactive.)

Section 4.1, which follows this introduction directly reviews the original concept for observing shafts of light formed as laser beams are scattered by coal dust particles. Section 4.2 examines the concept wherein the lasers intersect a plane of water to produce lighted points on that plane. Section 4.3 discusses techniques for determining z-axis position. Section 4.4 presents the second laser beam alternative to the coal dust and water plane techniques. Section 5 summarizes the characteristics of the three systems and outlines a design for the recommended system.

4.1 LIGHT SHAFT TECHNIQUE GEOMETRIES

Location of the shearer in x and y using the light shaft technique would be optimized if the sensor and the shafts were points on the same plane. The z-axis extent of the shafts is useful for ascertaining attitudinal data on roll, pitch and yaw, but not for position. The ideal situation of all points lying in a plane will be used in discussion of systems using a simple sensor station and one or more laser beams. It will be noted that little merit (but

much added cost and operation) accompanies the use of multiple sensors.

4.1.1 Single Laser Case

If the system has a sensor located at point P_s and an in-plane spot of light at P_1 . Determination of the single angle has no value in discovering the coordinates x and y . An infinite number of sets of x and y will satisfy the condition of constant θ defined by

$$\tan \theta = y_1/x_1.$$

Furthermore, without knowledge of the sensor (shearer) roll, the angle θ only relates to a shearer-based coordinate system, not to a tunnel-based system.

4.1.2 Two Laser Case

The ideal situation with two lasers is shown in Figure 2. Here two angles, θ_1 and θ_2 , are determined with respect to the sensor-based coordinate system. In the absence of roll, the sensor and tunnel coordinate systems are directly relatable. Otherwise, the shearer position still cannot be determined. The distance between the lasers, d_{12} , is known because this parameter is set on the fixed laser hardware at the end of the tunnel.

Analysis of the relationships between sides and angles of any plane triangle, particularly in the proof of the law of sines for

the circumscribed triangle of

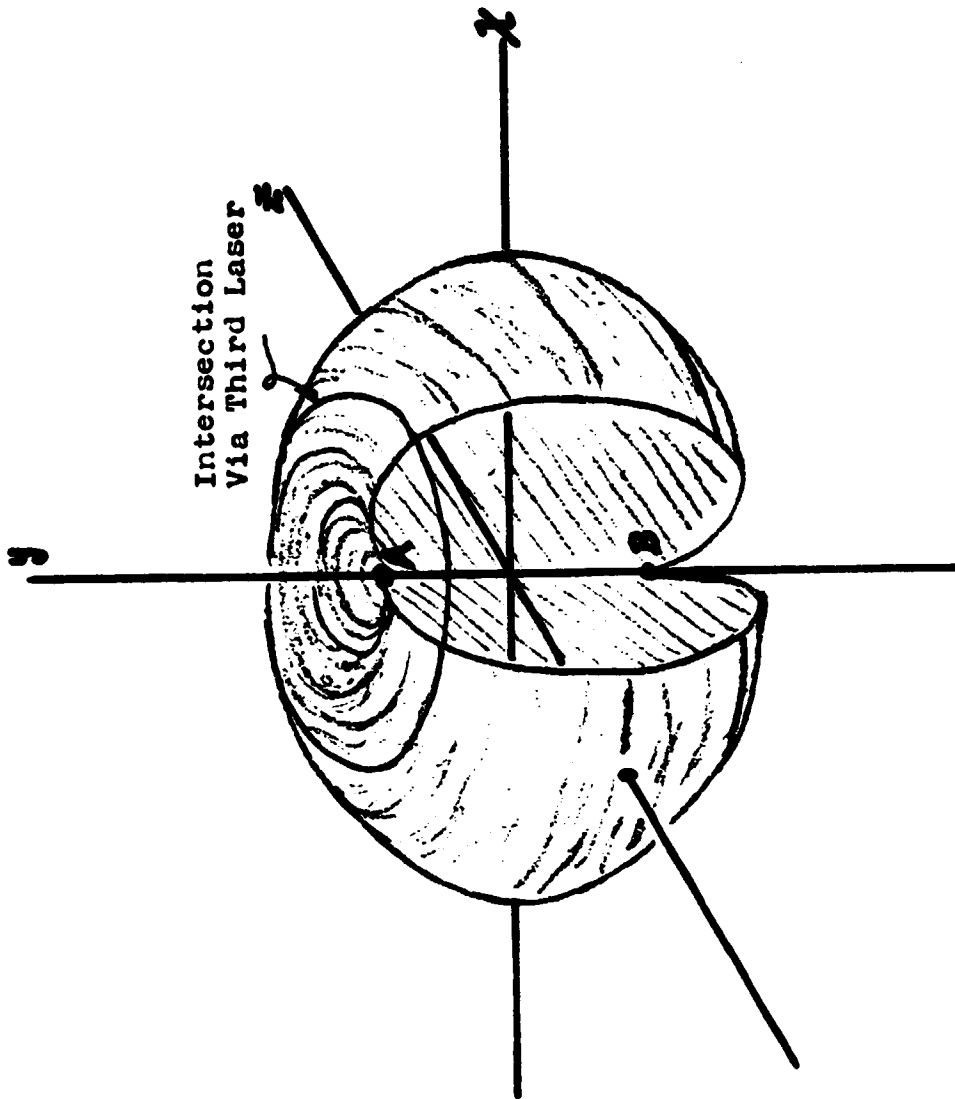
$$\frac{a}{\sin A} = \frac{b}{\sin B} = \frac{c}{\sin C} = \text{diameter of a circumscribed circle.}$$

In the two laser case the value of "a" is constant, being d_{12} . Therefore, for any given set θ_1 and θ_2 , shearer position can only be unambiguous if no roll is present. If roll is present, the sensor position can be anywhere on a circle where one triangle side is d_{12} . Emphasis should be placed on the fact that d_{12} need not be the diameter. Therefore, the general case is not a circle of ambiguity, but the intersected circles.

The situation is further complicated in the presence of pitch and yaw. Instead of circles of ambiguity, the surfaces of ambiguity suggested by Figure 29 exist. These are formed as surfaces of rotation of the ambiguity circles about the line between P_1 and P_2 .

4.1.3 Three Laser Case

The use of a third laser provides the added information to reduce the array of possible solutions of the two angular measurements. The added laser provides two additional circles of ambiguity. In the ideal planar case with no pitch and yaw, the position and the roll of the sensor can be determined by noting the only acceptable answer is obtained by the simultaneous solution of the three circles to find their common intersection, as shown in Figure 29. The presence of pitch and yaw complicates this, but can be handled by sequential observations along the z-axis as discussed later in



Intersection
Via Third Laser

Figure 29. Sketch of the Toroidal-like Ambiguity Surface for Observations of Points A and B.

ORIGINAL PAGE IS
OF POOR QUALITY

AS

Section 4.2.

4.1.4 Shafts versus Points

The actual implementation deals with shafts of light through points P_1 , P_2 and P_3 . The addition of a third dimension has an effect if the sensor tilts toward the beams. The shafts no longer appear parallel and spatial matching of the sensor IFOV (instantaneous field of view) to the light shaft becomes less effective.

4.2 TARGET PLANE TECHNIQUE GEOMETRIES

The original concept, described earlier, uses the offset observation of "lines" passing the photosensing system. The targets that produced these reference lines are coal dust particles distributed throughout a volume observable from the sensor position as limited by the view fields of the individual photodetector scans.

The problems with this approach included the following:

- (a) The signal strength of the laser light scattered by the coal dust particles is not detectable if MSHA standards are met.
- (b) The technique uses centroids of the laser line segments which may require temporal coding to keep sorted.
- (c) The geometry is not favorable to high accuracy.

In this section the possibility of avoiding these undesirable features will be examined using an alternate approach. This alternate approach is based on the observation of the intersection of the laser beams with a target plane. For simplicity in comprehending the discussions one might consider the beams striking a projection screen. This is only for understanding the involved geometries, however. Such a solid screen could not be placed in the system for reasons of mechanical damage, interference with mining activities and other practical considerations. A target plane that is practical, however, can be formed by water spray.

As has been the case throughout this analysis, the intent is to determine the several positional and attitudinal values for the shearer with an accuracy, and with a timeliness, appropriate to remote control. The discussion of the target plane technique in this section will adhere to these criteria, but extend them to their fuller meaning. Particular note will be made of the fact that mechanical realities keep the rates for pitch and yaw of the shearer track to values much less than roll. Because the desire is actually to control the orientation and trajectory of the shearer, the track parameters determine the fundamental characteristics needed for remote control. As long as these track parameters are determined at a rate coincident in z-axis movement resolution with the width of a roof support section, the location is effectively "instantaneous".

4.2.1 One Point on a Plane

In the absence of attitudinal variations (roll, pitch and yaw),

the shearer can be instantly located by observing a single laser beam crossing the target plane xy . Figure 3 illustrates this for a condition wherein the shearer is off the boresight coordinates. This simple case is not sufficient in the presence of roll, pitch and yaw.

The absence of roll allows the one-beam system to determine pitch and yaw by serial observations as the shearer moves along its rails. For example, an observation might be made at shearer position z and again at shear position $z + 5$ feet. The point P will change in x for a track that is yawed with respect to the tunnel. Changes along y will indicate track pitch.

Determination of pitch and yaw assumes that variations in these parameters is small over a distance of five feet due to the mechanical constraints of the shearer and track system. This suggests that determination of pitch and yaw at five foot intervals is tantamount to instantaneous determination. On the other hand, roll can be a rapidly changing parameter by comparison its companion angles (pitch and yaw). In the presence of this more rapidly changing parameter, unambiguous determination of shearer displacement is not possible in the single beam case.

4.2.2 Two Points on a Plane

The ambiguities associated with roll in the single beam case might be overcome by the use of a second beam. From the photosensing standpoint, this is equivalent to observation of two points in a

plane from a position out of that plane. Confusion of variables hurt two beam cases in the presence of roll, displacement, pitch and yaw. It is not possible with a single observation to separate these variables. Different combinations can produce the same coordinates.

The occurrence of yaw will result in an increase in the horizontal separation of the points P_1 and P_2 . This has an immediate effect on the perceived value of the roll angle Θ_R . Therefore, measurements require two sequential positions along the z-axis to determine pitch and yaw. Once these are determined, their effects can be backed out of the apparent displacement and roll calculations.

4.2.3 Three Points on a Plane

Three points on a plane can be shown adequate for determining displacements and the three angular coordinates with observation at a single z-axis location. However, as will be discussed later, the advantage of this approach over the two beam, two observation case is questionable. Accuracy and implementation may be higher in this later technique. Additionally, most favorable implementations do not use simultaneous detection of all points. Instead, sequential observations are made.

Consider the geometrical arrangement wherein the points in the xy plane are observed from an out-of-plane point. $P_0(0,0,z_0)$. The term z_0 indicates that the distance from the xy plane in this case is constant. Measurement of the theta (Θ) angles allows direct computation of the positions P_1 , P_2 and P_3 by basic trigonometry.

If the desired boresight positions of these three points are known, and if no roll is encountered, the shearer can be quickly located by coordinate subtractions. The presence of roll is readily detected by noting the three sets of subtractions will be different. In other words, if the shearer location is only translated in x and y, then the differences of the desired and measured positions can be grouped in sets $(\Delta x_1, \Delta y_1)$, $(\Delta x_2, \Delta y_2)$ and $(\Delta x_3, \Delta y_3)$. If no roll is present $\Delta x_1 = \Delta x_2 = \Delta x_3$ and $\Delta y_1 = \Delta y_2 = \Delta y_3$. However, when roll is encountered $\Delta x_1 \neq \Delta x_2 \neq \Delta x_3$ and $\Delta y_1 \neq \Delta y_2 \neq \Delta y_3$.

Location of the shearer in the presence of roll is accomplished by reestablishing the coordinate system. Rather than using sensor position P_0 as the origin of the xy plane, let the origin be the midpoint between the shearer wheels (as depicted in Figure 1) as they contact the guide rails. Cast into this coordinate frame the roll α is simply calculated by any combination similar to

$$\tan \alpha = \frac{\Delta y_2 - \Delta y_1}{\Delta x_2 - \Delta x_1}$$

After the roll is known its effect can be backed out by basic mathematics to obtain the offset in x and y.

As already mentioned, the shearer roll is obtainable from the determination of any two points that the reference laser beams intersect the xy plane. Obvious mechanical considerations relegate roll as the dominant attitudinal angle change possibility. Nevertheless, pitch and yaw can be cumulatively more significant even though their instantaneous magnitudes are likely to be far less

AS

than roll. These two additional attitudinal angles can be determined by obtaining the distances between observed points in each axial direction. If no pitch or yaw is present, then the separations in the x direction and the y direction will be the same as the established boresight reference beam separations. However, if yaw is encountered the separation of points in x will increase. Pitch will increase the separation of points in the y dimension. This is most easily seen graphically by using the selected coordinate system.

Changes in point separation along each axis are adequate to ascertain the magnitude of pitch and yaw, but are not sufficient to specify the direction of these changes in attitude. Specification of direction in the worst case arrangement requires two additional beams to provide references. In all cases, corrections for roll are made first. By noting which separations have the greater angular difference, the direction of the angle can be determined. The Cartesian coordinates difference should be the same for each set of points.

Fortunately, the worst case arrangement is not used for several reasons. Accordingly, the system does not require the three points to fit the axis of a Cartesian set. Therefore, something like an isocetes or equilateral triangle might be used. In either case the extra two beams can be dropped, allowing the return to a three beam system.

4.3 Z-AXIS DETERMINATION

The position of the sensor along the z axis is best determined opto-mechanically. One straightforward mechanical approach would count the cogging of the shearer along the track.* Another approach would use acoustic ranging. This second approach, would rely on optical signals to start a clock when a coded acoustic waveform is launched from the laser location. The time of arrival after the starting flash indicates the range, based on known propagation velocity for sound. The acoustic frequency would have to be high enough to allow directability, but low enough to avoid high absorption by atmospheric gases. Furthermore, frequency coding would be needed to improve signal-to-noise in the acoustically hostile region near the shearer. Operation from 50 KHz to 100 KHz with an LFM (linear frequency modulated) waveform is recommended. Compression would require either a tape loop or an incoherent optical processor.

4.4 LOCATION BY SCANNED LASER BEAMS

The scanned laser beam system uses mechanical determination of z-axis location and scanned laser beam angular measurements to determine shearer location. Trajectory attitudinal angles for pitch and yaw are ascertained by sequential position determinations. Roll is determined by angle separation of signals returned from two separated locations on the shearer body when scanned with a fanned laser beam.

*See Section 5 recommendations.

AS

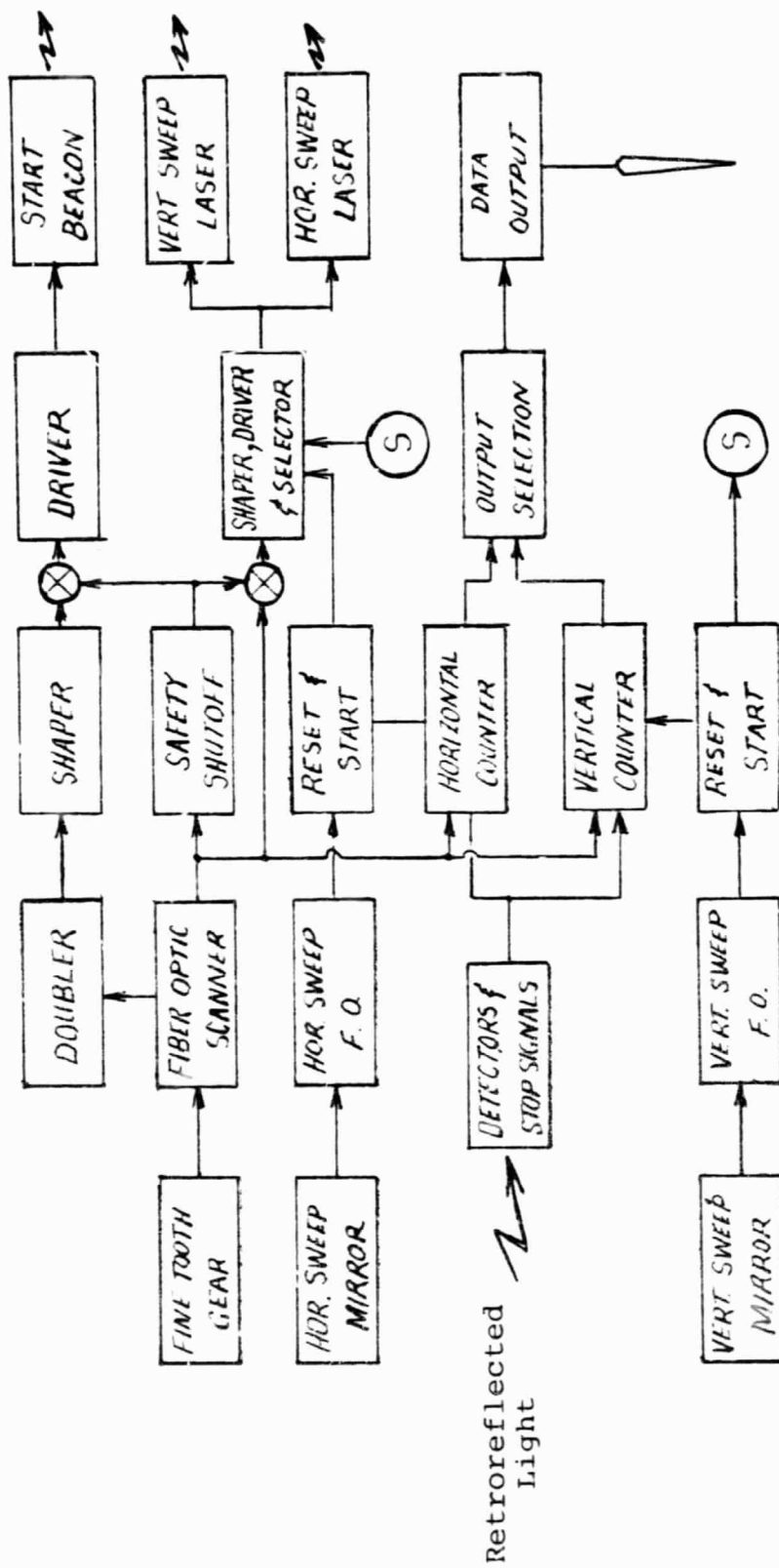
All electronic and optical devices, save for two retroreflectors on the shearer, could be housed in a single MSHA approved explosion proof box placed at one end of the longwall tunnel. The dimensions will be approximately 8" x 10" x 12". Low voltage gallium arsenide lasers would be used, but no laser safety glasses or goggles would be required by the miners. The table below summarizes realizable performance goals.

<u>Parameter</u>	<u>Value</u>
z-axis resolution	6 inches
y-axis resolution	6 inches
x-axis resolution	6 inches
Range	600 feet
Electronics package	8" x 10" x 12"
Input voltage	12 volts
Retroreflector package	5" x 2" x 16"

The system block diagram of Figure 30 shows the interrelationships of the functional elements. This figure will serve as reference for an outline description.

The fan-shaped laser beams are scanned by mirrors whose angular positions are determined by monitoring pulses from a fine tooth gear attached to the full speed shaft of the double shafted d.c. mirror drive motor. The low speed of the mirror motion is obtained from a motor-integral speed reduction box at the opposite end of the full

AS



SYSTEM BLOCK DIAGRAM

Figure 30

speed shaft. Accordingly, the full speed shaft will go through more than a hundred rotations for every rotation of the slow speed shaft. A fiber optic scanner monitors the passage of teeth on a gear as shown in Figure 31. The resultant pulses are fed to counters which sum the total number of pulses from the time the sweep mirrors are in a start position to the time the system photodetectors receive light reflected from the retroreflectors on the shearing machine.

Two counters are used. One for the horizontal sweep mirror and one for the vertical sweep mirror. The start position of each of these mirrors is indicated by fiber optic scanners which detect light reflected from the mirrors using the same type scanner as for the gear tooth monitoring. The mirror scan, in alternation, fan shaped beams vertically and horizontally over mechanically fixed angles. These beams are retroreflected from the shearer and stop the counter. The counted pulses give a high resolution indication of the angle moved from the reference position to the shearer position. Knowledge of the distance z gives an accurate indication of shearer position.

Figure 32 shows the synchronization of laser beam outputs and sweep angles. The top graph shows an optional wide angle strobe which can be used for optically obtaining a start signal to verify the mirror fiber optic scanner start signals and to assure that the shearer is actually in the optical line of sight if a stop signal is not found for the swept fan beams. This wide angle strobe is differentiated from the swept beams by doubling the frequency of its modulation relative to the swept beams. This checking option has a value which should be assessed after further study.

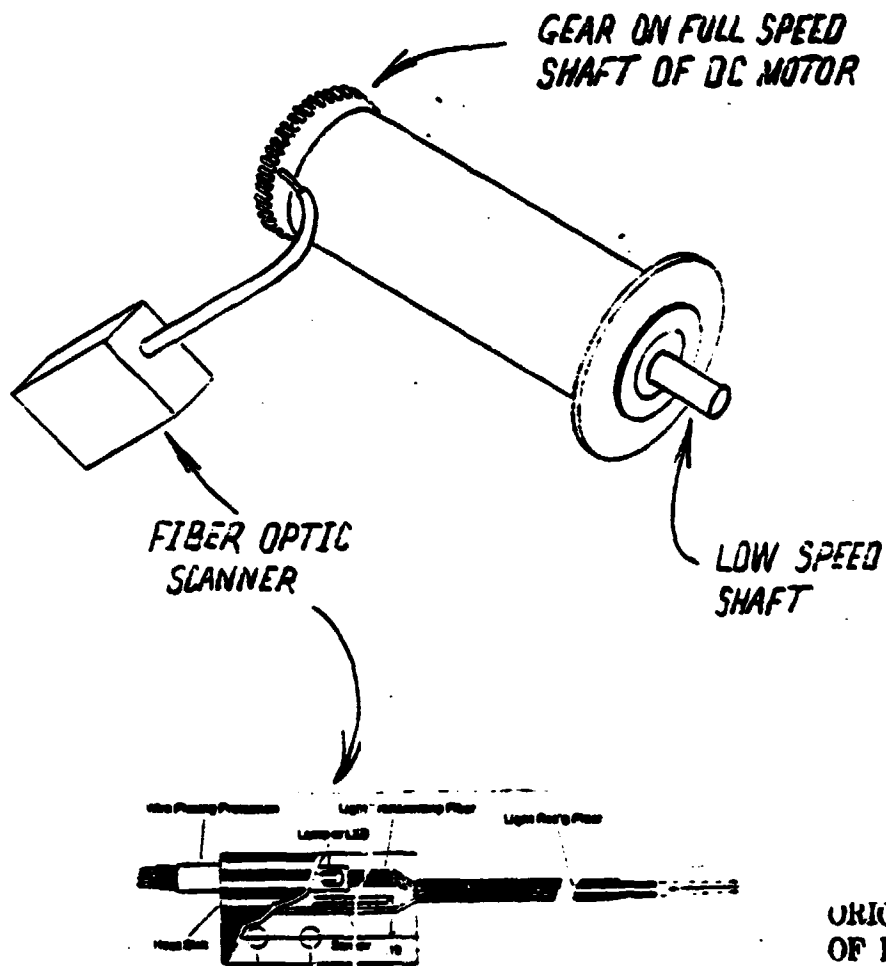


Figure 31 Technique for obtaining angular mirror position, providing laser modulation reference and regulating motor speed.

SYNCHRONIZATION

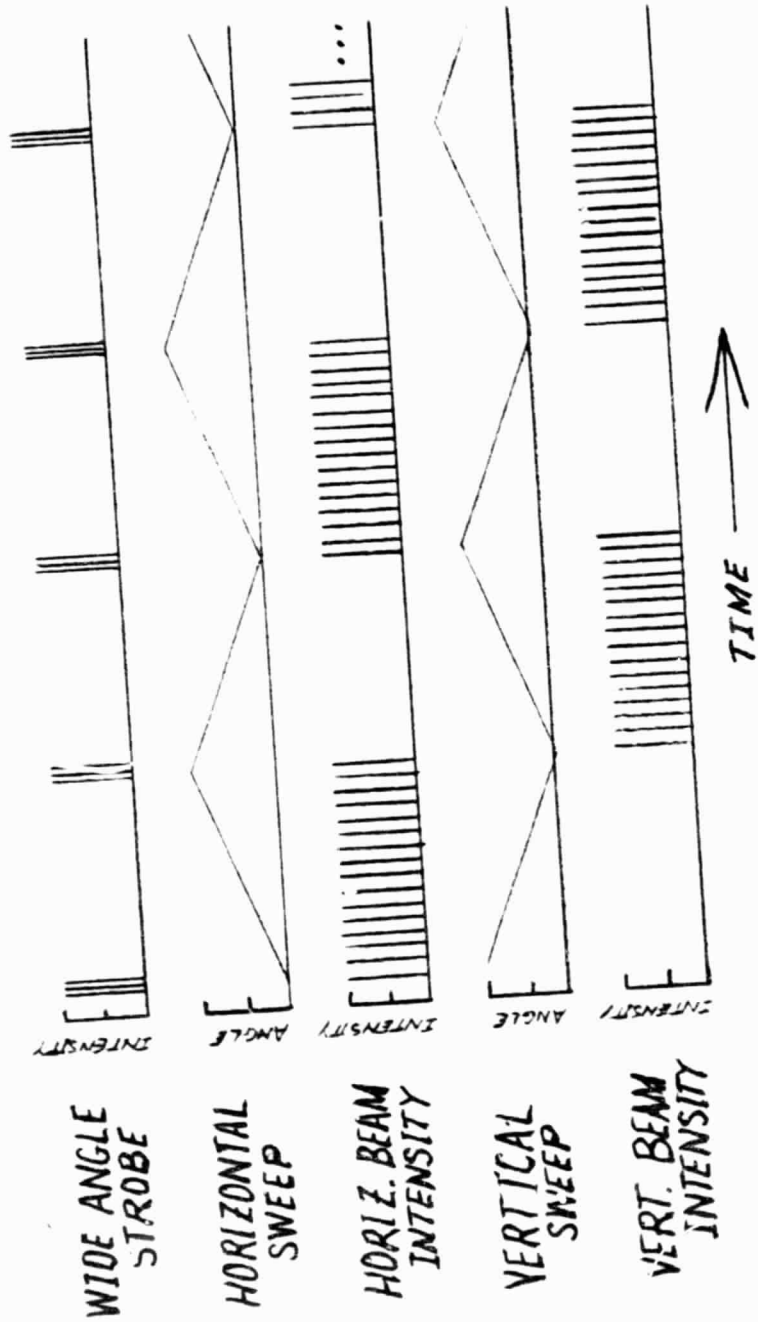


Figure 32 Synchronization Chart for the various optical outputs

AS

In order to avoid the use of safety goggles, the laser sweep action must be controlled in such a way as to insure the stop of sweep will immediately shut down the laser output. This is accomplished by requiring an input from the motor's five tooth gear rotation to drive the laser. Capacitive coupling between the gear signal and the laser driver might be used for this purpose. Furthermore, to guard against sweeping mirror stoppage independent of motor failure, consecutive counter start signals without associated stop signals will shut down laser driver power.

5. CONCLUSIONS & RECOMMENDATIONS

Three approaches have been analyzed for instantaneous determination of the trajectory of a longwall shearer as it progresses along its track. The section will summarize the significance of the results of those analyses. The summary will be comparative. That is, key aspects of each approach will be compared on a point by point basis.

The findings of the comparisons are essentially:

1. The initial concept based on coal dust scattering of boresighted laser beams is unfavorable for laser power, geometrical and safety reasons.
2. A variation on the initial concept would provide acceptable performance. This second approach, using water streams intersecting with boresighted laser beams, would require operators to wear safety goggles and HEW rule variance.
3. A third concept uses scanned laser beams instead of scanned sensors or targets. This approach is recommended. It is the least expensive and most reliable. Furthermore, more options exist for placement of the laser package, and no safety goggles are required.

The later part of this section presents a first order design for the recommended system.

5.1 CONCEPT COMPARISONS

5.1.1 Z-Location Systems

The down-tunnel position (z-location) of the shearer may be determined by counting cogs on the propelling mechanism, by monitoring the propagation time of an acoustic pulse transmitted from a reference location, and by triangulation using narrow beam optics. These possibilities are compared in the matrix of Table 4. The mechanical approach is clearly the most favorable on the sum basis of accuracy, simplicity, cost and safety. The sound delay technique would be acceptable. Triangulation is not favored, particularly with regard to accuracy.

5.1.2 XY-Location Systems

The shearer x- and y-axis locations (transverse axes looking parallel to longwall face) may be determined using fixed beam or scanned beam approaches. The fixed beam approaches are divided into techniques involving perpendicular observation of light scattered from suspended coal dust particles and techniques using nearly on-axis observation of light scattered from swept streams of water. The two scanned beam approaches are more closely alike. The principle difference resides in whether photodetectors or retroreflectors are attached to the shearer body.

Table 5 compares the four systems on a characteristic by characteristic basis. The support of this evaluation can be found in the text and the calculations of the preceding sections. In summary,

Z-LOCATION SYSTEMS

CONSIDERATION	USES		
	COG COUNTING	SOUND DELAY	TRIANG- ULATION
ACCURACY	1	1	3
SIMPLICITY	1	2	2
COST	1	2	2
SAFETY	1	1	1

KEY

- 1 FAVORABLE
- 2 ACCEPTABLE
- 3 UNFAVORABLE

Table 4 Comparison of Z-Location Systems

XY-LOCATION SYSTEMS

CONSIDERATION	FIXED BEAM		SCANNED BEAM	
	COAL PARTICLES	WATER PLANE	SENSOR DETECTOR	RETRO-REFLECTOR
TARGET CROSS-SECTION	3	2	1	1
DATA ADEQUACY	2	1	1	1
PENETRATION OF MEDIUM	1	1	1	1
SCANNING COMPLEXITY	3	2	1	1
OPTICAL COMPLEXITY	3	1	1	1
OPTICAL-MECH. ENVIRONMENT	2	2	1	1
SAFETY (*NO GOGGLES)	2	1	1*	1*

Table 5 Comparisons of XY-Location Systems

the table suggests that the study has shown unfavorable characteristics for the coal particle concept with regard to signal levels and implementation characteristics. The water stream approach is clearly acceptable, but the scanned beam techniques are overall more favorable yet. Either scanned beam technique is appropriate. However, the system recommended later (Section 5.2) uses retro-reflectors. This eliminates the need to electrically communicate signals from shearer to the tunnel end. In fact, no electronics need be installed on the shearer at all for this approach.

5.1.3 Attitude Determining Systems

Table 6 compares the four xy-location systems with regard to their abilities to determine the attitudinal angles of roll, pitch and yaw. The use of a mechanical leveling readout device is also shown for comparison.

The level sensor is favored for roll and pitch determination at any given location. It should be noted, however, that since the desired information is more appropriately trajectory, the instantaneous data might need low-pass digital filtering. The optical systems stack up for roll and yaw approximately as they did for x and y.

Analysis results are unfavorable for yaw-determination by either mechanical or coal dust scattering techniques. While the mechanical level concept is useful for roll and pitch, it is not valid for yaw because there is no gravitational force in yaw. Such

ATTITUDE DETERMINING SYSTEMS

CHARACTERISTIC	MECHANICAL		FIXED BEAM		SCANNED BEAM	
	LEVEL		PARTICLE	WATER	DETECTOR	REFLECTOR
ROLL						
ACCURACY	1*		2	1	2	2
SIMPLICITY	1		3	2	1	1
COST	1		3	2	1	1
SAFETY	1		2	1	1	1
PITCH						
ACCURACY	1		2	1	1	1
SIMPLICITY	1		3	2	1	1
COST	1		3	2	1	1
SAFETY	1		2	1	1	1
YAW						
ACCURACY	3		2	1	1	1
SIMPLICITY	3		3	2	1	1
COST	3		3	2	1	1
SAFETY	1		2	1	1	1

1=FAVORABLE 2=ACCEPTABLE 3=UNFAVORABLE

*BASED ON REQUIREMENTS FOR TRAJECTORY CORRECTIONS

Table 6 Comparison of Attitude Determining Systems

force would have to be induced by machine movement in the xz-plane. Recording such movement with accelerometers and processing the data appropriately would be an overtaxing endeavor.

The use of the coal dust scattering technique in yaw determination is undesirable for the same unfavorable reasons cited on earlier applications. Overall, the scanned laser approaches are most favorable.

5.2 RECOMMENDED SYSTEM

If z-axis distance is known, then the x- and y-axis displacements can be determined from horizontal and vertical angular measurements between some boresight line and a reference point on the shearer. The simplest approach would be to observe the shearer body with a video camera. Allowing that some place on the shearer could be made clearly apparent by increased brightness compared to the rest of the machine, the video raster signal could be easily processed to indicate the two needed angles. Two difficulties arise, however. One is practical realization of the bright fiducial. The other concerns the desirability of using an image tube (or even charge transfer array) in the coal mine.

A light emitting diode (LED) might be placed on the machine body. An appropriate narrow band filter in the sensor optics would then assure a very large contrast ratio between the LED and any other part of the machine. Unfortunately, this highly preferred approach is not usable in the near term due to the realities of the time

required for mine certification. The current schedule for the NASA Mineral Extraction Office necessitates being on line for demonstration in approximately six months. Given enough time to develop and obtain certification on the right package, however, would pay great dividends in location design simplicity, and in transmission of data.

Current designs for the various NASA-sponsored longwall instruments use a data transmission cable between the shearer machine and the control station. The use of a machine mounted light emitting diode*, with modulation electronics, would allow transmission of data without any objectionable cables! The same sensor used to obtain the horizontal and vertical angles could also monitor the data modulations. Therefore, even though time may not allow certification of a machine mounted, solid state light emitting diode for an early demonstration, any system that is used for a demonstration should allow the eventual evolution of such operation.

Now, the same certification reality exists for the sensor as exists for the source. At least the system is not complicated by machine mounting. Nevertheless, certification of any new electronics in the short time frame would be difficult. One must seek some usage of already acceptable gear in a demonstration that would make it unchallengably clear that a design concept would work. It is improbable that any electronic video equipment could ever be

*Note: Since an LED is not a laser, Bureau of Radiological Health certification is avoided.

assembled, let alone certified in the time frame. Even if such were possible, the acceptability and maintainability of video equipment by the coal mines is doubtful for the very near future. Furthermore, a video-based system has a very limited, fixed upper bound of resolution elements. Zoom optics, with tracking, would be required to overcome this limit for circumstances of the shearer moving from close to far. Finally, without intensifier stages, video cameras have far less sensitivity than individual photo-detectors. For these and additional reasons a mechanically swept scanning process is recommended. A viable scanning process would incorporate a fanned beam.

The difficulties for near term demonstration of this concept arise not only from hardware component availability, but also from the same certification lead time that plagues the previous discussion. This leaves one to ask "Can I make a totally convincing demonstration of the preferred concept using already accepted devices in such a way that only the slightest modification would be needed to configure it for a certified electronic version?" Adjunct Systems has thought and puzzled over this problem. It now feels a positive "Yes" answer is possible.

The solution centers around a second question. "Even if we had an electronic demonstrator, what use would the output be?"

END DATE

~~NOV~~ NOV. 4, 1981

AS